UNIVERSITÉ DU QUÉBEC À RIMOUSKI

Étude multi-traceurs de la productivité primaire et du paléoclimat dans le nord de la baie de Baffin

Mémoire présenté

dans le cadre du programme de maîtrise en océanographie

en vue de l'obtention du grade de maître ès sciences

PAR

© **Marc-André Cormier**

Avril 2013

UNIVERSITÉ DU QUÉBEC À RIMOUSKI
Service de la bibliothèque

Avertissement

Composition du jury :

Jean-Carlos Montero Serrano, président du jury, Université du Québec à Rimouski

André Rochon, directeur de recherche, Université du Québec à Rimouski

Anne de Vernal, codirecteur de recherche, Université du Québec à Montréal

Yves Gélinas, codirecteur de recherche, Université Concordia

Simon Belt, examinateur externe, University of Plymouth

Dépôt initial le 18 janvier 2013   Dépôt final le 24 avril 2013

how many years
can a mountain exist
Before it's washed to the sea?

REMERCIEMENTS

X

RÉSUMÉ

Cette étude lie les changements de la productivité primaire et les conditions marines de surface dans le nord de la baie de Baffin depuis 1560 AD à partir d'une carotte de sédiments récoltée à l'été 2008. Des reconstitutions quantitatives des conditions marines de surface, dérivées d'assemblages de kystes de dinoflagellés et de fonctions de transfert utilisant la technique des analogues modernes (MAT), ont été combinées à la composition isotopique du carbone et de l'azote et à l'analyse des biomarqueurs organiques. Plus particulièrement, IP_{25} (Ice Proxy avec 25 atomes de carbone) et les dinostérols ont été analysés. IP_{25} est un isoprénoïde hautement ramifié (*higly branched isoprenoïd*, ou HBI) apparemment produit par une diatomée vivant dans la glace de mer, genre *Haslea*, alors que le dinostérol est un stérol principalement produit par des dinoflagellés. Nos résultats montrent un climat relativement stable, avec deux intervalles de productivité primaire maximale et un léger réchauffement depuis 1560 AD. Par ailleurs, nos reconstitutions quantitatives des conditions marines de surface utilisant la MAT suggèrent que le biomarqueur IP_{25} est plus utile pour évaluer la productivité primaire que la concentration de glace de mer dans un environnement de glace de mer relativement stable. Finalement, notre étude montre un écosystème dominé par les diatomées en interaction avec la glace de mer, où le couvert de glace semble être le principal facteur limitant la productivité primaire depuis 1560 AD.

Mots clés: productivité primaire, baie de Baffin, dinoflagellés, reconstitutions, biomarqueurs, IP_{25}, dinostérol, diatomées, composition isotopique

ABSTRACT

This study links the evolution of primary productivity and sea-surface conditions in northern Baffin Bay since 1560 AD from a sediment core collected in the summer of 2008. Quantitative reconstructions of sea-surface conditions derived from dinoflagellate cyst assemblages and transfer functions using the Modern Analogue Technique (MAT) were combined with the stable isotope composition of organic carbon and nitrogen and the concentration of organic biomarkers (IP_{25}, Ice Proxy with a 25 carbon atom skeleton and dinosterol) in bulk sediment. IP_{25} is a highly branched isoprenoid (HBI) produced in the Arctic Ocean by the sea-ice diatom *Haslea ostrearia*, whereas dinosterol is a sterol produced mainly by dinoflagellates. Our results show a relatively stable climate with two intervals of maximum primary productivity and a slight warming since 1560 AD. Moreover, comparison between quantitative reconstitutions of sea-surface conditions using MAT and organic biomarkers results indicate that IP_{25} could be more useful in evaluating the primary productivity in a sea-ice environment (e.g. stable ice-edge conditions) than the fluctuations of the sea-ice cover. Finally, the region shows an ecosystem dominated by diatoms in close interaction with the sea-ice, in which temperature seems to be the main factor controlling primary productivity since 1560 AD.

Keywords: Baffin Bay, Arctic, quantitative reconstruction, dinoflagellate, isotopic composition, transfer function, biomarkers, dinosterol, IP_{25}

TABLE DES MATIÈRES

LISTE DES TABLEAUX

MULTY PROXY STUDY OF PRIMARY PRODUCTIVITY AND PALEOCLIMATE IN NORTHERN BAFFIN BAY, CANADA

LISTE DES FIGURES

INTRODUCTION GÉNÉRALE

LISTE DES ABRÉVIATIONS, DES SIGLES ET DES ACRONYMES

ACIA   Arctic Climate Impact Assessment

APP   Annual Primary Productivity

GIEC   Groupe d'experts Intergouvernemental sur l'évolution du Climat

IPCC   Intergovernmental Panel on Climate Change

IAPP   International Arctic Polynya Program

IP$_{25}$ Ice Proxy with a 25 carbon atom skeleton

IHO   International Hydrographic Organization

IBCAO   International Bathymetric Chart of the Arctic Ocean

MAT   Modern Analogue Technique

NODC   National Oceanographic Data Center

SIP   Sea Ice Presence

SST$_a$ Sea Surface Temperature in August

INTRODUCTION GÉNÉRALE

L'Arctique et le réchauffement climatique

L'Océan Arctique, au sens strict, correspond à un bassin interne excluant la baie de Baffin et la mer du Groenland (Menard et Smith, 1966; Jakobsson, 2002; Jakobsson *et al.*, 2003). Toutefois, les mers arctiques incluent, de façon plus générale, l'ensemble de la surface océanique délimitée par le cercle polaire arctique (66°33'44''N) (IHO, IBCAO), soit la contrée du soleil de minuit. À ces latitudes extrêmes, le faible angle d'incidence des rayons solaires résulte en un climat très froid. Ainsi, la majeure partie du territoire est recouverte par la glace et la neige lui donnant un albédo très élevé. En conséquence, la plus grande partie de l'énergie solaire est réfléchie vers l'atmosphère (ACIA, 2004).

De ce climat extrême, il résulte un écosystème caractérisé par des espèces spécialisées et donc très vulnérables aux variations climatiques (Parmesan, 2006), mais jouissant toutefois d'une valeur intrinsèque (Ghilarov, 2000; Costello *et al.*, 2010). Malgré son isolement et sa vulnérabilité, l'Arctique joue un rôle central dans le système terrestre en raison de son implication dans plusieurs phénomènes d'envergure planétaire (par exemple, albédo et bilan d'énergie terrestre, bilan d'eau douce et circulation thermohaline, réservoir d'hydrates de gaz, grandes migrations aviaires, biodiversité) (ACIA, 2004; IPCC, 2007). Toutes ces raisons font de la compréhension de l'Arctique une région d'étude prioritaire.

Il est difficile de bien comprendre l'écosystème arctique et la biosphère en général, car nos connaissances limitées des variations climatiques à long terme nous font voir notre monde comme étant stable ou à l'équilibre, alors qu'il est en changement continuel. Il est donc primordial d'établir des repères fixes afin d'évaluer son évolution. La paléocéanographie nous permet justement d'estimer de tels changements à des échelles de temps géologiques.

Étudier le passé de la Terre est le seul moyen à notre disposition nous permettant d'établir un véritable principe de réfutabilité (Popper, 1963) pour tester des hypothèse en écologie globale. Lorsque des phénomènes se produisent à des échelles de temps millénaires, étudier le passé devient le seul moyen de tester les théories tentant de les expliquer. Par exemple, l'étude du passé de la Terre pourrait constituer le meilleur outil pour comprendre les possibles régulations homéostasiques de la biosphère (Lovelock, 1993).

Au cours des dernières années, la communauté scientifique internationale a noté un réchauffement sans équivoque du climat. Dans son rapport publié en 2007, le Groupe d'experts Intergouvernemental sur l'Évolution du Climat (IPCC, 2007) affirme que 11 des 12 dernières années figurent parmi les plus chaudes depuis 1850, année à laquelle les relevés instrumentaux ont commencé (Figure 1). Le groupe estime d'ailleurs que le réchauffement global enregistré a été de 0,74 °C depuis 1906 et que c'est en Arctique que le réchauffement est le plus élevé. Le groupe d'évaluation des impacts d'un réchauffement de l'Arctique (ACIA, 2004) indique d'ailleurs que le réchauffement de l'Arctique a été de 0,90°C entre 1900 et 2003.

En parallèle au réchauffement observé, une hausse des concentrations des gaz à effet de serre, imputable aux activités humaines, a aussi été notée durant la même période et serait responsable du réchauffement observé. Les concentrations de CO_2 atmosphérique ont augmenté de 280 ppm (parties par million) depuis l'époque préindustrielle à 379 ppm en 2005 (IPCC, 2007) et de nos jours à 396 ppm (ProOxygen, 2013), ceci en plus des autres facteurs jouant un rôle certain dans l'évolution du climat, notamment les cycles de Milankovitch, l'activité solaire et l'activité sismique et volcanique (IPCC, 2007).

Pour bien comprendre le rôle de chaque phénomène, mesurer l'importance relative du réchauffement actuel et surtout comprendre comment l'écosystème peut s'adapter à de tels changements, il est nécessaire d'étudier le passé de la Terre, particulièrement celui de l'Arctique qui semble avoir un rôle clef dans le système planétaire.
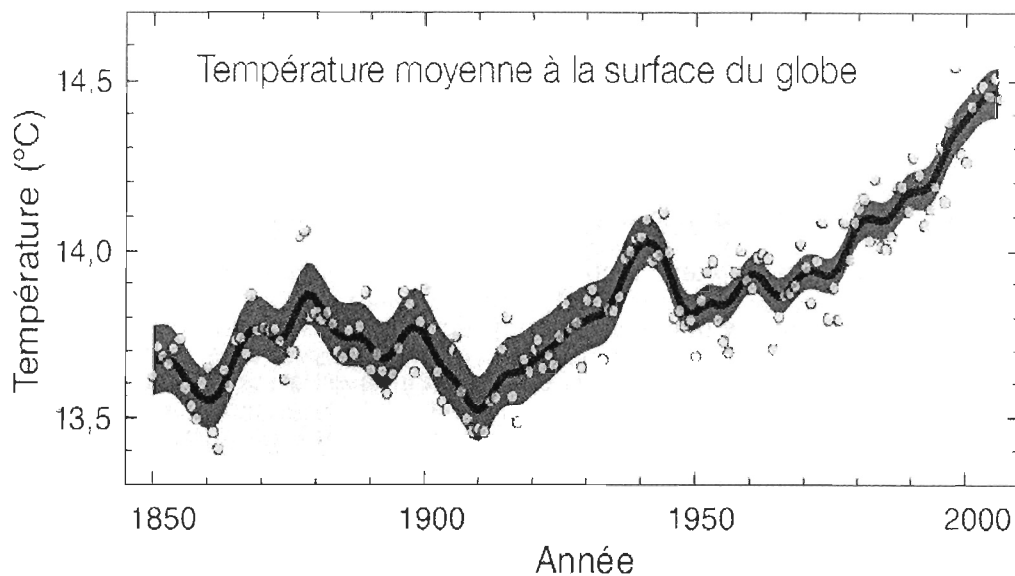
Figure 1. Variations de la température moyenne à la surface du globe depuis 1850. La courbe lissée représente les moyennes décennales, et les cercles correspondent aux valeurs annuelles. La zone en bleu représente les intervalles d'incertitude qui ont été estimés à partir d'une analyse détaillée des incertitudes connues (Modifiée de GIEC/IPCC, 2007).

La polynie des Eaux du Nord et la baie de Baffin

Les efforts pour comprendre les réponses de l'écosystème arctique aux variabilités interannuelles et aux changements climatiques ont mené à l'étude des polynies. Dans le nord de la baie de Baffin, la polynie des Eaux du Nord a été l'objet de travaux dans le cadre du projet de recherche North Water Polynya (NOW) entre 1990 et 2002, projet qui s'insérait dans le cadre d'un programme international sur les polynies arctiques (International Arctic Polynya Programme, IAPP). La majeure partie des données recueillies durant le projet NOW sont disponibles en ligne à l'adresse suivante: http://www.quebec-ocean.ulaval.ca/now/.

La zone de $5\text{-}8 \cdot 10^4$ km^2 constituant les Eaux du Nord est illustrée à la Figure 2. Cette région montre régulièrement des étendues libres de glace au début du mois d'avril contrairement au reste de l'archipel arctique canadien qui n'en montre habituellement qu'à la mi-juillet (Fortier et al., 2002). Les vents et les courants dominants venant du nord, et,

dans une moindre mesure, les eaux plus chaudes provenant du courant ouest groenlandais ainsi qu'une résurgence au sud-est de la région seraient responsables de cette ouverture rapide de la banquise au printemps (Barber *et al.*, 2001; Melling *et al.*, 2001).

Plusieurs études montrent que le secteur des Eaux du Nord est l'une des régions les plus productives du cercle polaire arctique (e.g. Tremblay *et al.*, 2006). La région est d'ailleurs l'objet de floraisons massives (bloom) de diatomées au printemps (Lewis *et al.*, 1996). De plus, la présence des Inuits près de cette région est associée à la présence d'une mégafaune aquatique. Le possible lien de causalité entre la forte productivité de la région et la présence d'une mégafaune (Dunbar, 1981), de même que le devenir du carbone organique produit dans les eaux de surface représentaient les thèmes principaux du programme NOW et plus récemment du programme ArcticNet. Les résultats suggèrent que la forte productivité planctonique de la polynie soutient la faune pélagique herbivore mais ne contribue pas de façon majeure à la pompe biologique à CO_2. Par ailleurs, le devenir du carbone organique dissous issu de la production biologique dans les eaux de surface et sa transformation ultérieure demeurent incertains (Tremblay *et al.*, 2006).

C'est dans ce contexte qu'une campagne d'échantillonnage paléocéanographique a été entreprise dans la baie de Baffin à l'été 2008 afin d'évaluer les changements environnementaux de la région au cours des derniers milliers d'années. Dans ce projet de maîtrise, une carotte par boîte prélevée à proximité de la polynie des Eaux du Nord a été analysée afin de caractériser l'évolution du climat et de la productivité primaire dans la région au cours du passé récent.

Les indicateurs paléocéanographiques

Il existe plusieurs indicateurs paléocéanographiques pouvant aider à reconstituer l'évolution des environnements marin arctiques (de Vernal *et al.*, 2008). Il y a les traceurs sédimentologiques, indépendants de la production biologique et purement reliés aux processus sédimentaires (par exemple, la granulométrie) (McCave, 2007; de Vernal *et al.*, 2008). Il y a les traceurs géochimiques, telle la composition isotopique de la glace ($\delta^{18}O$ et

δ^2H), des tests carbonatés de foraminifères (δ^{18}O et δ^{13}C) et de la matière organique (δ^{13}C, δ^{15}N et δ^2H) (Hillaire-Marcel *et al.*, 2004). Il y a également les traceurs biogéniques, comprenant les microfossiles (par exemple, coccolithes, tests de foraminifères, frustules de diatomées, squelettes de radiolaires, kystes de dinoflagellés, grains de pollen et spores), ainsi que les biomarqueurs organiques (par exemple, les alkénones, les chlorines, le dinostérol, IP_{25}), qui sont des molécules identifiables dans les particules sédimentaires, et initialement produites par des organismes vivants (Rontani *et al.*, 2007; Rosell-Melé et McClymont, 2007).
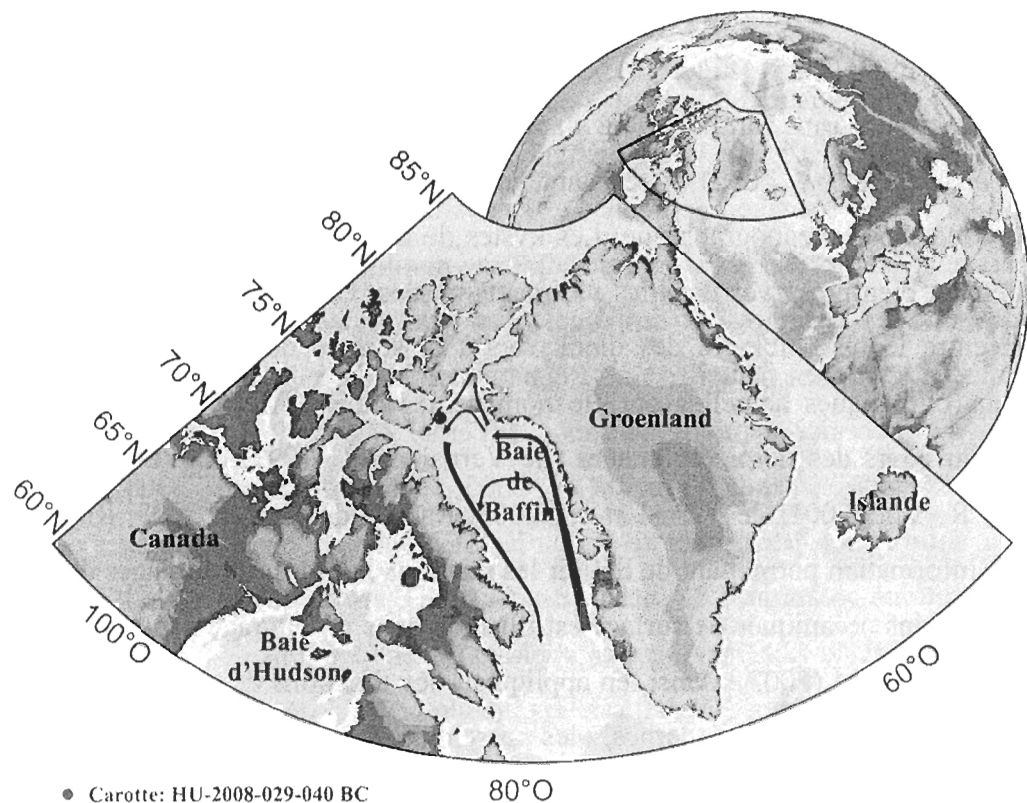
Figure 2. Carte de localisation de la zone d'étude dans la baie de Baffin, Haut Arctique canadien. Le point rouge représente l'endroit où la carotte (HU-2008-029-040 BC, 46 cm) a été prélevée à la position (75,58° N, -78,63° O). La profondeur de l'eau à cet endroit est de 580 m. La zone en bleu représente la polynie des Eaux du Nord. Flèches rouges: courant relativement chauds; flèches bleues: courants froids

Les kystes de dinoflagellés

Les kystes produits par les dinoflagellés (dinokystes) sont parmi les microfossiles les plus intéressants à étudier dans un contexte de marge continentale des milieux de hautes latitudes. En effet, les dinoflagellés (Dinophyceae) sont des organismes unicellulaires auto, hétéro- ou mixotrophes responsables d'une part importante de la production primaire en milieu marin (Menden-Deuer et Lessard, 2000). Ils sont avec les diatomées des contributeurs majeurs à la chaîne alimentaire marine (Tappan, 1980), et sont présents en grande quantité de l'équateur aux pôles et des zones néritiques à océaniques ouvertes. Environ 15 % des dinoflagellés produisent un kyste (hypnozygote) organique durant leur cycle de vie (Evitt, 1985) (Figure 3). Ce kyste, produit suite à la fusion des gamètes, est composé de dinosporine, un polymère s'apparentant à la cellulose (Versteegh et Blokker, 2004; Versteegh *et al.*, 2012) et résistant aux processus diagénétiques, peut être utilisé comme traceur paléocéanographique. Les kystes de dinoflagellés ainsi produits sont donc généralement bien préservés dans les sédiments marins. Des études visant à déterminer la relation entre les assemblages des dinokystes à la surface des sédiments marins et les conditions climatiques actuelles ont été nombreuses dans l'Arctique et dans les hautes latitudes au cours des dernières années (de Vernal *et al.*, 1997; de Vernal *et al.*, 2001; Mudie et Rochon, 2001; de Vernal *et al.*, 2005; Radi et de Vernal, 2008; Richerol *et al.*, 2008). L'information permettant de définir les relations liant les assemblages de dinokystes et les conditions océaniques de surface est illustrée dans un ouvrage synthèse présenté par Marret et Zonneveld (2003). Ainsi, en appliquant des fonctions de transfert, notamment la méthode des analogues modernes, les assemblages de dinokystes permettent la reconstitution des conditions marines de surface (salinité, température, glace de mer, et productivité primaire) dans les milieux arctiques (de Vernal *et al.*, 2001; de Vernal *et al.*, 2005; de Vernal et Hillaire-Marcel, 2008; de Vernal *et al.*, 2008; Ledu *et al.*, 2008; Radi et de Vernal, 2008; Rochon *et al.*, 2008; Ledu *et al.*, 2010a; Ledu *et al.*, 2010b).
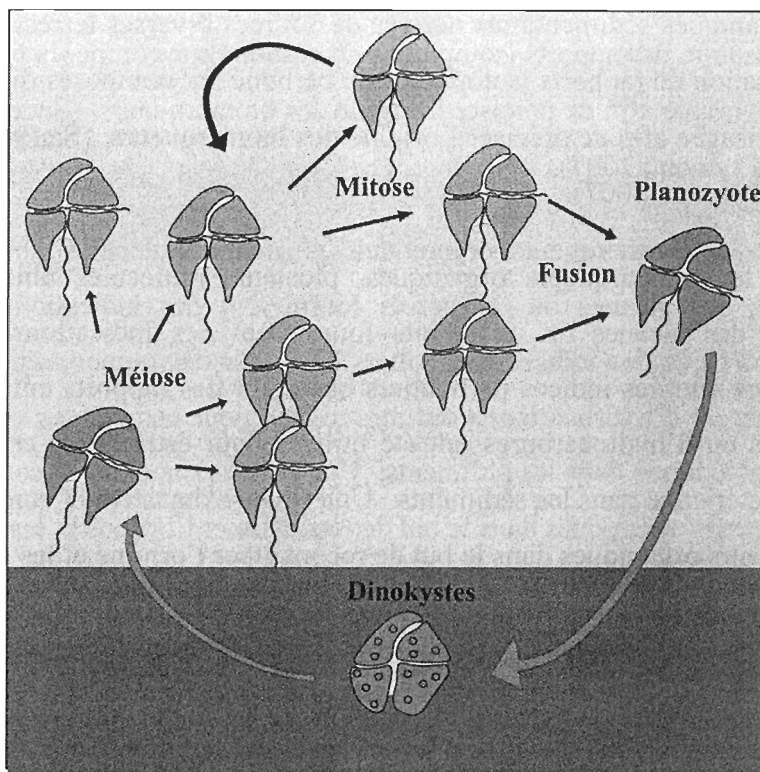
Figure 3. Représentation simplifiée du cycle de vie des dinoflagellés. Adaptée de Evitt (1985).

Biomarqueurs organiques

Parmi les traceurs biogéniques, certains biomarqueurs ont aussi montré un fort potentiel paléocéanographique pour l'Arctique. Comme ils peuvent transiter longtemps avant d'être ensevelies dans les sédiments marins, il est très important de bien comprendre les mécanismes sédimentaires impliqués dans leur dépôt (par exemple, adsorption, absorption, transport vertical et latéral par le vent, les vagues et les glaces, le remaniement sédimentaire), car ceux-ci peuvent avoir des conséquences importantes sur leur interprétation subséquente (Belicka *et al.*, 2004; Rosell-Melé et McClymont, 2007; Belicka *et al.*, 2009).

La porté paléoécologique des biomarqueurs peut être vérifiée par l'utilisation croisée de différents traceurs (Henderson, 2002). Par exemple, l'utilisation de biomarqueurs d'origine connue permet de diminuer l'incertitude inhérente associée à l'utilisation de

substrats organiques sédimentaires dérivés de sources diverses terrestres et aquatiques. En outre, l'utilisation de rapports isotopiques du carbone sur composés organiques spécifiques peut être envisagée afin de préciser l'origine des biomarqueurs (Sauer *et al.*, 2001; Rosell-Melé et McClymont, 2007).

Parmi les biomarqueurs organiques, plusieurs molécules ubiquistes dérivées des acides gras, des alcanes ou de stérols fournissent des indications sur la productivité primaire, alors que des indices particuliers basés sur des rapports entre différents groupes d'acides gras ou d'hydrocarbures ont été utilisés pour estimer les contributions terrestre, marine et bactérienne dans les sédiments. Une revue exhaustive et complète de l'utilisation de biomarqueurs organiques dans le but de reconstituer l'origine et les transformations de la matière organique sédimentaire a été publiée par Peters *et al.* (2005).

Plus spécifiquement, le dinostérol, produit majoritairement par les dinoflagellés, permet d'évaluer l'apport des dinoflagellés dans les sédiments marins. Comme la plupart des stérols, cette molécule est relativement bien conservée dans les sédiments marins. La somme de ses produits de dégradation connus, incluant le dinostanol, le dinostérone et le dinostanone, semble être étroitement corrélée avec l'abondance de dinokystes dans les sédiments marins (Mouradian *et al.*, 2007).

Finalement, l'IP$_{25}$ (*Ice Proxy with a 25 carbon atom skeleton*), un hydrocarbone mono-insaturé apparemment produit par une diatomée vivant dans les glaces (genre *Haslea*), semble avoir le potentiel de retracer les conditions de glace de mer. En effet, cette molécule est bien conservée dans les sédiments et n'a été retrouvée jusqu'à maintenant que dans les environnements caractérisés par une couverture saisonnière de glace de mer (Belt *et al.*, 2007). Par ailleurs, des travaux récents ont démontré que la production par les diatomées du genre *Haslea* est dépendante des concentrations en nutriments et non de la concentration de glace de mer (Lavoie *et al.*, 2010). D'ailleurs, jusqu'à maintenant aucune étude n'a pu établir de lien entre les quantités d'IP$_{25}$ retrouvées dans les sédiments et la concentration de glace de mer (ou le pourcentage de couverture par la glace) dans les eaux

associées. Ce projet de recherche tente d'établir ce lien par le biais d'une approche multi-traceur.

Objectifs spécifiques et contributions

L'objectif de ce projet de recherche est de retracer l'évolution des conditions océaniques de surface et de productivité primaire dans la polynie des Eaux du Nord au cours des derniers siècles (~500 ans) à partir d'une séquence sédimentaire de 46 cm de longueur.

Pour chaque centimètre de la séquence sédimentaire (46 échantillons), l'analyse de biomarqueurs (alcanes, acides gras, chlorines, stérols, IP_{25}) et de traceurs géochimiques ($\delta^{13}C$, $\delta^{15}N$) a été combinée aux reconstitutions quantitatives des conditions de surface obtenues à partir des assemblages de kystes de dinoflagellés et de fonctions de transfert utilisant la méthode des analogues modernes.

La productivité primaire a été caractérisée en utilisant les traceurs spécifiques disponibles. Soit les biomarqueurs organiques, la composition isotopique de la matière ($\delta^{15}N$ et $\delta^{13}C$) organique ainsi que la méthode des analogues modernes appliquée sur les assemblages de dinokystes.

En parallèle, des analyses du biomarqueur IP_{25} ont été réalisées afin d'établir des comparaisons avec les reconstitutions basées sur les assemblages de dinokystes dans le but de vérifier sa fiabilité pour retracer la concentration de glace de mer.

J'ai réalisé toutes les analyses à l'exception de celles du biomarqueur IP_{25}. Les traitements palynologiques ont été effectués dans le laboratoire de palynologie de l'Institut des sciences de la mer de Rimouski (UQAR/ISMER), alors que l'analyse des palynomorphes a été réalisée dans le laboratoire micropaléontologie du GEOTOP à l'Université du Québec à Montréal.

Toujours au GEOTOP, la chronostratigraphie de la séquence sédimentaire a été obtenue par la mesure du ^{210}Pb et du ^{226}Ra dans les laboratoires de radiochronologie. Les âges AMS-^{14}C ont été effectués au Lawrence Livermore National Laboratory.

Les analyses de biomarqueurs organiques et d'isotopes stables ont été faites à l'Université Concordia dans le laboratoire environnemental de géochimie organique.

Finalement, l'analyse du traceur IP$_{25}$, a été effectuée en collaboration par le Dr Guillaume Massé au Laboratoire d'Océanographie et du Climat (LOCEAN) à l'université Pierre et Marie Curie (France).

MULTY PROXY STUDY OF PRIMARY PRODUCTIVITY AND PALEOCLIMATE IN NORTHERN BAFFIN BAY, CANADA

1. INTRODUCTION

1.1. THE ARCTIC AND GLOBAL WARMING

The Arctic plays a central role in the Earth's system because of the role it is playing in several major global phenomena (e.g., albedo and energy balance, freshwater balance and ocean conveyor belt, gas hydrates and hydrocarbon reservoirs, large bird migrations, biodiversity) (ACIA, 2004; IPCC, 2007). These reasons make understanding the Arctic a priority issue. It is therefore essential to establish fixed reference points to evaluate its evolution and paleoceanography allows doing it over geological time scales.

In recent years, the international scientific community and the Intergovernmental Panel on Climate Change (IPCC, 2007) have unequivocally noted a warming of the climate. The group estimates that the global warming recorded was up to 0.74°C since 1906 and that the greatest warming is taking place in the Arctic for an increase of 0.90°C in the same period (ACIA, 2004). Parallel to the observed warming, an increase in greenhouse gas concentrations caused by human activities was also observed, in addition to other factors playing a definite role on climate, more specifically the Milankovitch cycles, solar, seismic and volcanic activity (IPCC, 2007). To measure the importance of the current warming and above all, to comprehend how the ecosystem can adapt to such changes, it is essential to study the Earth's past, particularly that of the Arctic that appears to have a key role in the planetary system.

1.2. PALEOCEANOGRAPHY OF THE ARCTIC

1.2.1. North Water Polynya and northern Baffin Bay

Efforts to understand the response of arctic ecosystems to interannual variability and climate change have led to the study of polynyas. In northern Baffin Bay, North Water Polynya was the target of a research project (NOW) between 1990 and 2002 within the scope of the International Arctic Polynya Program (IAPP). The majority of data collected during the NOW project are available online at the following address: http://www.quebec-ocean.ulaval.ca/now/. It is also presently studied has part of ArcticNet, a Network of Centres of Excellence of Canada.

The zone of $5\text{-}8 \cdot 10^4$ km^2 forming the North Water Polynya is illustrated on Figure 4. This region regularly shows ice-free waters in early April, whereas the rest of the Canadian Arctic Archipelago shows similar conditions only around mid-July (Fortier *et al.*, 2002). Currently, the mean sea ice cover is about 7.9 months yr^{-1} within the polynya, whereas it is about 11.2 months yr^{-1} in the remaining Canadian Arctic Archipelago. The prevailing winds and currents from the north, and less importantly, the warmer water from the West Greenland Current (WGC) upwelling in the eastern part of the polynya are all responsible for the rapid opening of the sea-ice in the spring (Barber *et al.*, 2001; Melling *et al.*, 2001).

Several studies summarized by Tremblay *et al.* (2006) show that the North Water is one of the most productive regions of the Arctic. The region is also subject to massive diatom blooms in the spring (Lewis *et al.*, 1996). Moreover, the presence of the Inuit people in that region is associated to the presence of aquatic megafauna (e.g. whales, seals and walruses).

The possible causal link between the high primary productivity of the region and this presence of the megafauna (Dunbar, 1981), as well as the fate of the organic carbon produced in surface waters, were the main focus of the NOW program. Results have shown that the high plankton productivity in the polynya supports the pelagic herbivore fauna, but the fate of dissolved organic carbon (DOC) derived from biological production in surface

waters of the North Water Polynya and its subsequent transformations remain uncertain (Tremblay *et al.*, 2006).
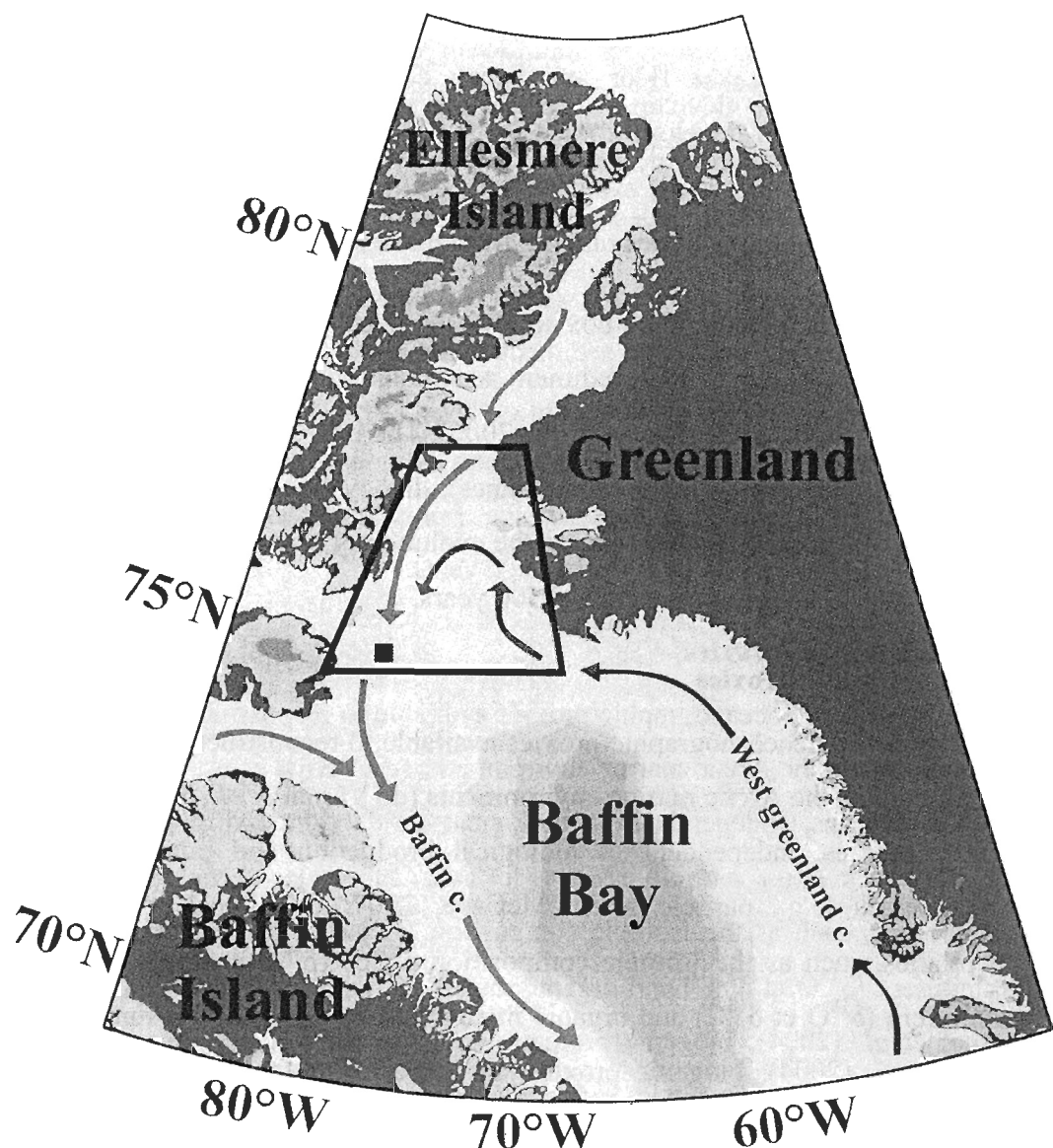
Figure 4. Location of the study area in Baffin Bay, Canadian High Arctic. The black box indicates the location of the 46 cm-long core HU-2008-029-040 BC (75.58°N, -78.63°W, water depth = 580 m). The black quadrilateral represents the North Water Polynya. The red arrows represent the West Greenland Current while the blue arrows the Baffin Island Current.

The paleoceanographic campaign HU-2008-029 was undertaken in that context in summer 2008 across Labrador Sea and Baffin Bay in order to sample both the water column and bottom sediments to (i) quantify the relationship between particle fluxes (biogenic and detrital) to the sea floor and ocean conditions (productivity, current, temperature, salinity, etc.), (ii) develop proxies for the reconstruction of changes in sea-surface conditions or currents, and (iii) evaluate changes in both the climate and ocean in the eastern Canadian Arctic at time scales ranging from hundreds to thousands of years.

For this thesis project, a 46 cm-long box core was collected at the western edge of the North Water Polynya at a site with high sediment accumulation rates ranging around 0.05 to 0.19 cm yr^{-1} (Hamel *et al.*, 2002; Mudie *et al.*, 2006). The box core was analyzed for its organic biomarkers content (IP$_{25}$, sterols, and alkanes), dinocyst assemblages and isotopic composition ($\delta^{15}N$ $\delta^{13}C$) in order to characterize the evolution of sea-surface conditions and primary productivity in that region over the last 500 years.

1.2.2. Paleoceanographic proxies

There are several paleoceanographic proxies available to reconstruct the evolution of sea surface conditions in the Arctic marine environments (de Vernal *et al.*, 2008). There are sedimentological proxies, independent of biological production and purely related to sedimentary processes (e.g., particle size) (McCave, 2007; de Vernal *et al.*, 2008); geochemical proxies, such as the isotopic composition of ice ($\delta^{18}O$ and δD), calcareous tests of foraminifera ($\delta^{18}O$ et $\delta^{13}C$) and organic matter ($\delta^{13}C$, $\delta^{15}N$ and δD) summarize in Hillaire-Marcel *et al.* (2004); biogenic proxies, including microfossils (e.g., coccoliths, tests of foraminifera, diatom frustules, radiolarian skeletons, dinoflagellate cysts, pollen and spores), and organic biomarkers (e.g., alkenones, chlorines, dinosterol, IP$_{25}$), recognizable molecules in the sedimentary records, and originally produced by living organisms (Rontani *et al.*, 2007; Rosell-Melé et McClymont, 2007).

1.2.3. Dinoflagellate cysts

Cysts produced by dinoflagellates (dinocysts) are among the most useful microfossils in high latitude and continental margins areas. Dinoflagellates (Dinophyceae) are unicellular protists, hetero- or mixotrophic and are responsible for a significant proportion of primary productivity in the world oceans (Menden-Deuer et Lessard, 2000). They are major contributors to the marine food chain, following the diatoms (Tappan, 1980), and are present in large quantities from the equator to the poles, as well as from the open ocean to neritic zones. Approximately 10-15% of dinoflagellates produce an organic cyst (hypnozygote) during their life cycle, after the fusion of gametes. The cyst is composed of dinosporine, a polymer similar to cellulose (Versteegh *et al.*, 2012), known to be very resistant to diagenic degradation processes. Dinoflagellate cysts are thus well preserved in marine sediments and can be used as a paleoceanographic proxy (e.g. Evitt, 1985). Studies to determine the relationship between dinocyst assemblages of surface sediments and current climate conditions have been numerous in the Arctic and at high latitudes in recent years (de Vernal *et al.*, 1997; de Vernal *et al.*, 2001; Mudie et Rochon, 2001; de Vernal *et al.*, 2005; Radi et de Vernal, 2008; Richerol *et al.*, 2008). Modern reference databases were used to define the relationships between dinocyst assemblages and sea-surface parameters such as sea ice cover, temperature, salinity and primary productivity. By applying the Modern Analogue Technique (MAT), dinocyst assemblages allow the reconstruction of marine surface conditions (salinity, temperature, sea ice, and primary productivity) in Arctic environments (de Vernal *et al.*, 2001; de Vernal *et al.*, 2005; de Vernal et Hillaire-Marcel, 2008; de Vernal *et al.*, 2008; Ledu *et al.*, 2008; Radi et de Vernal, 2008; Rochon *et al.*, 2008; Ledu *et al.*, 2010a; Ledu *et al.*, 2010b).

1.2.4. Organic Biomarkers

Organic biomarkers are widely used biogenic proxies (Volkman, 2003) and have also shown their potential for paleoceanography in the Arctic.

The reliability of biomarkers can be verified through the use of multiple proxies (Henderson, 2002). For example, the use of organic biomarkers of known origin can reduce

the uncertainty associated with the use of sedimentary organic substrates derived from various terrestrial and aquatic sources.

However, they can remain in the water column a long time before being buried in marine sediments. Therefore, it is important to further study the mechanisms involved in their sedimentary deposition (e.g., adsorption, absorption, transport by vertical and lateral currents, waves and ice, sediment reworking) because these mechanisms can have important consequences on their interpretations (Belicka *et al.*, 2004; Rosell-Melé et McClymont, 2007; Belicka *et al.*, 2009).

Among the organic biomarkers, several ubiquitous molecules derived from fatty acids, alkanes or sterols provide information on primary productivity, while individual indices based on ratios between different groups of fatty acids or hydrocarbons were used to estimate the terrestrial, marine and bacterial contributions to the sediments. A broad review of the use of organic biomarkers to reconstruct the origins and transformations of sedimentary organic matter was published by Peters *et al.* (2005).

More specifically, dinosterol (Figure 5b) is produced mainly by dinoflagellates although also by certain diatoms and allows tracing the contribution of dinoflagellates to the sterol content in marine sediments. Like most sterols, this molecule is relatively well preserved in marine sediments. The sum of its known degradation products, dinostanol, dinosterone and dinostanone appears to be closely correlated with the abundance of dinocysts in marine sediments (Mouradian *et al.*, 2007).

Finally, IP_{25} (Ice Proxy with a 25 carbon atom skeleton, Figure 5a), a highly branched isoprenoid (HBI) produced by diatoms, apparently from *Haslea* genus, seems to have the potential to track sea-ice conditions. Indeed, this molecule is well preserved in sediments and it has only been found in seasonal sea-ice environments (Belt *et al.*, 2007). However, recent studies have shown that primary production by diatoms (mostly from the genus *Haslea*) depends mainly on nutrient concentrations rather than sea-ice concentration (e.g. Lavoie *et al.*, 2010). Moreover, no study links the amount of IP_{25} in sediments and the sea-

ice cover (or the sea ice concentration) in the associated water. This study has attempted to establish this link through a multi-proxy approach.

a)   b)
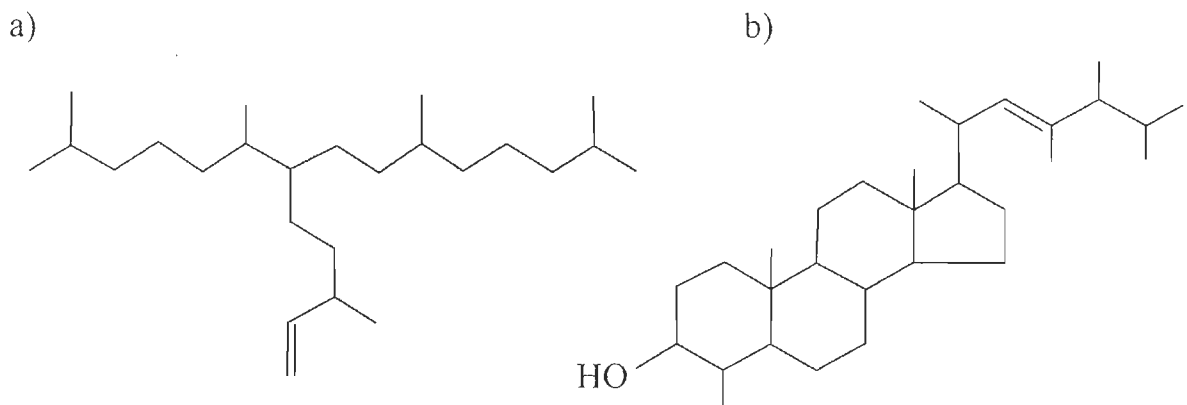
Figure 5. Chemical structure of a) IP$_{25}$ b) Dinosterol

1.3. SPECIFIC OBJECTIVES

This research presents a multi-proxy study designed to compare two sea-ice proxies, IP$_{25}$ and MAT using dinoflagellate cyst assemblages, in order to reconstruct the changes of sea-surface conditions and primary productivity over the last 500 years in northern Baffin Bay using a 46 cm-long box core collected at the western edge of the North Water Polynya.

The 46 cm-long core was subsampled at 1 cm intervals and each sample was analysed for organic biomarkers (alkanes, sterols, IP$_{25}$) and geochemical tracers ($\delta^{13}C$, $\delta^{15}N$), combined with quantitative reconstructions of sea-surface conditions, obtained from dinoflagellate cyst assemblages and transfer functions using the modern analogs technique.

Sea-surface physico-chemical parameters (temperature, salinity, duration of sea-ice, primary productivity) were documented using dinocysts and organics biomarkers as proxies.

2. MATERIEL AND METHOD

2.1. SAMPLING

A box core (2008-029-040 BC ; 46 cm in length) was collected at 580 m water depth, at the western edge of the North Water Polynya in northern Baffin Bay (75.58° N, 78.63° W, Figure 1) during the oceanographic campaign 2008-029, which was carried out between August 28 and September 23, 2008, aboard the Canadian Coast Guard Ship (CCGS) Hudson. Three pushcores (A, B and C) were sub-sampled from the box core. Pushcore A was archived and pushcore B was sampled every cm. Each subsample was divided into three fractions (palynological, isotopic and organic geochemical measurements). Pushcore C was used to analyse the physical properties of the sediments (P-wave velocity, magnetic susceptibility, electrical resistivity and gamma density) using a multi sensor core logger, and the analysis of the remanent magnetism. The pushcores and subsamples were stored at 4°C. A fraction (15 cm^3) of each subsample from sequence B was stored at -20°C for the analysis of organic biomarkers.

2.2. CHRONOSTRATIGRAPHY OF THE SEDIMENTARY SEQUENCE

The chronostratigraphy of the sedimentary sequence B was determined from fifteen ^{210}Pb measurements performed in Geotop center and three AMS-^{14}C dating of carbonate shells achieved by the Lawrence Livermore National Laboratory. The total activity profile of ^{210}Pb (^{210}Pb$_{tot}$) in the sediments was inferred by measuring the daughter element, ^{210}Po, using an α spectrometer. Figure 6a illustrates the activity of supported ^{210}Pb (^{210}Pb$_{sup}$), which was deduced from the activity of ^{226}Ra (in secular equilibrium) measured by γ spectrometry. The "excess" ^{210}Pb, or unsupported (^{210}Pb$_{exs}$), was obtained by subtracting the supported fraction (^{226}Ra) from ^{210}Pb$_{tot}$ following the approach proposed by Laissaoui *et al.* (2008).

The sedimentation rate calculated assuming constant flux and constant sedimentation (CF-CS) method is 0.17 cm yr^{-1}, while it is 0.10 cm yr^{-1} when using the constant rate of

supply (CRS) method (Sorgente, 1999) (Figure 6b). The ^{210}Pb data and calculations are reported in Annexe I (Table 3).

The sedimentation rate obtained from the CRS method (0.10 cm yr^{-1}) was used for the determination of the chronostratigraphy of the sedimentary sequence because it is compatible with the ^{14}C measurements by accelerator mass spectrometry (AMS) on bivalve shell fragments (Figure 6c; Table 1).
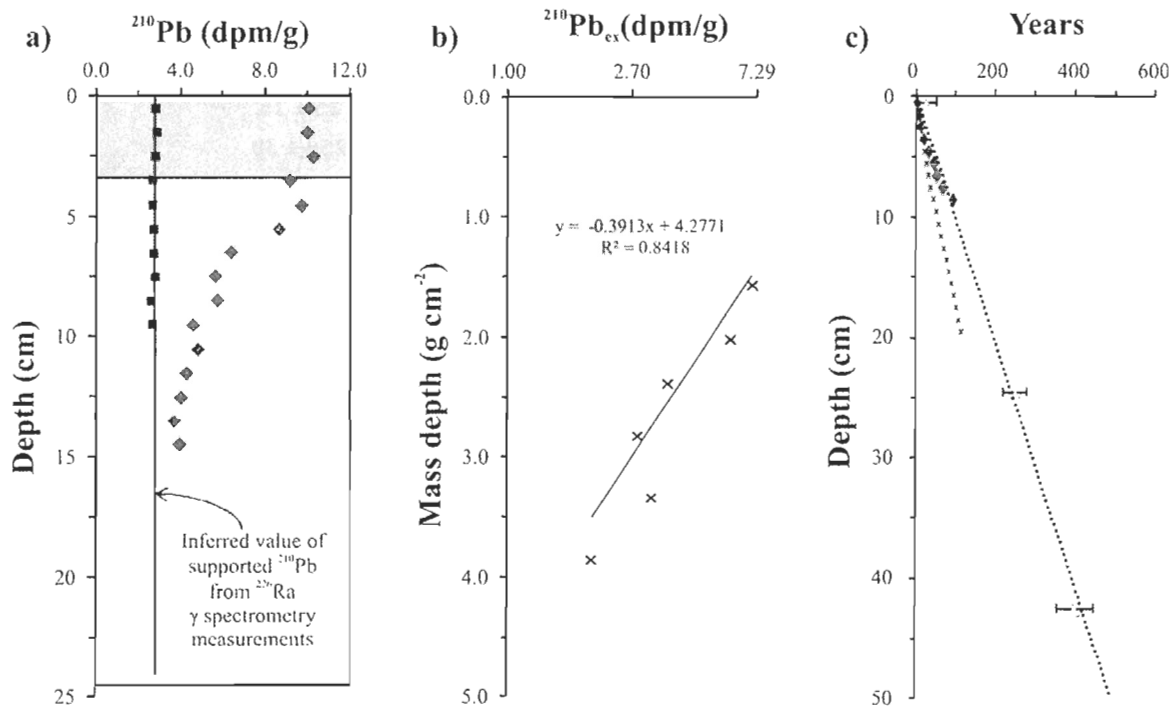
Figure 6. a) Load ^{210}Pb data and estimate sedimentation rates. Blue diamonds and red squares represent ^{210}Pb and ^{226}Ra activities respectively. The black line represents supported ^{210}Pb given by ^{226}Ra activity. The gray zone represents the mixing zone b) Neperian logarithm of excess ^{210}Pb used to estimate the mean sediment accumulation rate of 0.078 g cm^{-2} y^{-1} using the constant flux-constant sedimentation method (CF-CS). c) Blue squares and black circles represent constant rate of supply (CRS) and extrapolated CRS ages, respectively, black crosses represent the CF-CS ages and green triangles represent the ^{14}C ages.

Three radiocarbon ages were calibrated using the software Calib 6.1.1 (Table 1). The regional difference from the average global marine reservoir correction (ΔR) used is 222 ± 16 years and is based on the mean of the five calibration points closest to the box core and

available in the marine reservoir correction database (Stuiver, 2011). In agreement with the sedimentation rate obtained from ^{210}Pb measurements, the sedimentation rate obtained from the ^{14}C ages is about 0.11 cm yr^{-1} and appears to be uniform throughout the sedimentary sequence.

Table 1. Radiocarbon ages used to corroborate sedimentation rate obtained from ^{210}Pb measurements.

Depth	Material dated	Laboratory numbers	Conventional radiocarbon ages	Calibrated ages[a]
cm			BP	cal BP
0-1	Bivalves	150982	> Modern	25 ± 25
24-25	fragments	150983	810 ± 30	250 ± 30
42-43	shell	150984	975 ± 30	401 ± 46

[a]Calibrated ages were estimated using the software Calib version 6.1.1 with a ΔR local reservoir effect of 222 ± 15 years (confidence interval of 0.69 and 0.93) (Stuiver 2011).

2.3. PALYNOLOGICAL ANALYSES

2.3.1. Sample preparation and microscopy

Each sample was treated using a standardized palynological treatment method as described by Rochon *et al.* (1999). Approximately 5 cm^3 of wet sediment was sieved through two Nitex® membranes of 100 and 10 μm. A capsule of *Lycopodium clavatum* spores with a known concentration (12,100 ± 1892 spores/tablet: batch #414831) was added to the samples before sieving to assess the palynomorph concentrations, which are expressed as number of cyst per gram of dry sediment (cyst g^{-1} dry sediment). The sediment fraction between 10 and 100 μm was treated with hot hydrochloric acid (HCl 10%, 4 times for 10 min) to dissolve carbonate particles, alternating with hot hydrofluoric acid (HF 49%, 2 times for 10 min and 1 time for 12 h) to dissolve silica particles. The residue obtained was sieved again on a 10 μm Nitex® membrane. A few drops of phenol were added to the residue for the preservation, which was then stored at 4°C. Part of this fraction was mounted in a glycerin gel for a systematic counting of at least three hundred palynomorphs with a transmitted light microscope (Leica® 5500B) at 400× magnification.

2.3.2. Dinoflagellate cyst nomenclature

Dinocyst taxa were identified using the identification keys presented in Rochon et al. (1999) and in Radi *et al.* (2013). The identification key of Radi *et al.* (2013) is particularly appropriate for the Arctic because it improves the identification of problematic round brown spiny cysts such as *Echinidinium karaense* vs. *Islandinium* spp., which are abundant in arctic regions.

2.3.3. Paleoenvironmental reconstructions

Quantitative estimates of past sea-surface parameters were reconstructed from dinocyst assemblages using the Modern Analogue Technique (MAT) as described by Guiot et Goeury (1996) with the R software using the procedure described by de Vernal *et al.* (2005). MAT was performed using one of the latest version of the GEOTOP reference database (n=1429) (de Vernal *et al.*, 2005). The best estimates, which correspond to the average weighted inversely to the distance for the five best analogues, were calculated with respect to a set of five best modern analogues. Modern environmental data used for reconstruction consist in sea-surface temperature and salinity values at 10 m depth provided by the 2001 version of the World Ocean Atlas (NODC, 2001). Seasonal duration of sea-ice cover, defined as the number of months per year with sea-ice coverage greater than 50%, was compiled using the 1953–1990 data set provided by the National Climate Data Centre in Boulder, Colorado. Primary productivity was computed from satellite observations from the MODerate resolution Imaging Spectroradiometer (MODIS) program (observations from 2002 to 2005). By dividing the database into verification and calibration data sets, validation tests performed on the 'n=1429' database permit to assess on the error of prediction. Relationships between estimates and observations are linear, with high correlation coefficients: August Sea-Surface Temperature (SST_a): R^2=0.96; August Sea-Surface Salinity (SSS_a): R^2=0.76; Sea-Ice Cover (SIC): R^2=0.87; Annual Primary Productivity (APP): R^2=0.81). Standard deviation of the residuals (RMSE: Root Mean Square Error) provides an estimation of the accuracy of reconstructed parameters; they are

±1.7°C, ±2.3 PSU, ±1.4 months yr^{-1} and ±57.7 gC cm^{-2} yr^{-1} for SST$_a$, SSS$_a$, SIC and APP, respectively.

2.4. ISOTOPIC GEOCHEMISTRY

The organic carbon (C$_{org}$) and nitrogen (N) content and their isotopic ratios (δ^{13}C, δ^{15}N) were measured in the sediments with an Elemental Analyzer (EA) coupled to an isotopic ratio mass spectrometer (IRMS). An aliquot of each sample was dried and grinded before being analyzed. For each sample, a first aliquot was weighed into a tin capsule and analyzed directly for its total N content. A second aliquot was weighed in a silver capsule before being placed in an acidic atmosphere (HCl vapour) for 12 hours to remove the carbonates. Subsequently, each treated aliquot was placed in a second tin capsule and analyzed for C$_{org}$ and δ^{13}C. β-alanine was used as the calibration standard and the standard deviation on the measures were ±0.08% for C$_{org}$, ±0.01% for N, ±0.2‰ for δ^{13}C and finally ±0.3‰ for δ^{15}N.

2.5. ANALYSIS OF ORGANIC BIOMARKERS

2.5.1. Sample preparation

IP$_{25}$ analyses was carried out by Dr Guillaume Massé (Université Pierre et Marie Curie, France) as described previously in Belt *et al.* (2007). For other compounds, 30 g of dry sediment from the frozen fractions of each subsample from pushcore B were treated. Immediately after addition of an internal standard solution containing n-docosane-d$_{46}$, n-octadecyl-d$_{37}$ and pentadecanoic-d$_{29}$ acid (Sigma-Aldrich®), the total lipid fraction was extracted in Teflon tubes with a solution of 2:5:2 MeOH:CHCl$_3$:H$_2$O by mechanical shaking for 2 hr following a 30-min sonication step. The extraction was repeated 3 times for a minimum of 2 hr each time. The organic phase was collected and filtered through a glass wool-filled pipette to remove residual particles. The total extract was then dried under a gentle stream of nitrogen (N$_2$), and the total lipid extract was saponified with 5 mL of a solution of 5 N KOH in methanol and 1 mL of distilled water. The mixture was refluxed for 2 hr and the organic phase was extracted 3 times in a 5% NaCl solution in dichloromethane

(DCM). The saponified lipids were filtered and dried under N_2. The saponified lipid fraction was re-dissolved 3 times in 200 μL of a hexane-toluene solution (25 %) and 3 times in 200 μL of methanol (100 %) and separated into a polar and a non-polar compound fractions using long column silica gel chromatography. Non-polar lipids (e.g., hydrocarbons) were eluted with a hexane-toluene solution (25 %), whereas the more polar lipids, including fatty acids, alkanols and sterols, were eluted with methanol (100 %). The sterol fraction was derivatized with trimethylsilyl in a 1:1 solution of N, O-bis (trimethylsilyl) trifluoroacetamide (BSTFA) and pyridine at 80°C during 1 hr before injection in the gas chromatograph, while the hydrocarbons were injected without pre-derivatization.

2.5.2. Sample analyses

The samples were directly injected in a Varian Saturn CP-3800/2200 ion trap Gas Chromatograph – Mass Spectrometer (GC-MS) for compound identification. The GC was fitted with a splitless injector set at 310°C and a DB-5ms column. For the analysis of non-polar lipids, the initial oven temperature was set at 90°C and ramped to 250°C at 20°C min^{-1}, then ramped to 310°C at 1°C min^{-1} and finally held at the final temperature for 10 min. For the analysis of the sterol fraction, the initial oven temperature was set at 120°C, ramped to 310°C at 3°C min^{-1} and held at this temperature for 10 min. The transfer line to the MS detector was set at 310°C, the manifold at 50°C and the trap at 80°C for the non-polar lipids and at 120°C for polar lipids. Individual compounds were identified on the basis of comparison between their GC retention times and mass spectra with those of authentic standards mixtures of sterols and alkanes (Sigma-Aldrich®) as described previously in Mouradian *et al.* (2007).

The samples were also injected in an Agilent 6890N Gas Chromatograph – Flame Ionization Detector (GC-FID) using the same parameters (and a FID temperature of 325°C) to quantify the compounds of interest. The concentrations, expressed in micrograms per gram of organic carbon (μg gC^{-1}), were calculated by comparing the intensity measured for each peak of interest to those of standards injected under the same chromatographic

conditions and corrected for differences in the recovery of the internal standards. The precision of the overall procedure (extraction, purification, derivatization, and GC analysis) were estimated through the analysis of three aliquots of a natural and spiked (100 mg L^{-1} equivalent of the standard sterol mixture in the final solution) sediments collected in the Saguenay Fjord (Quebec, Canada) in May 2002. The precision and accuracy were estimated previously at ±15% (Mouradian *et al.*, 2007).

3. RESULTS

3.1. ISOTOPE GEOCHEMISTRY

The C_{org} content records a slight increase in C_{org} from 2.05 to 2.43 % from the bottom to the top of the core (Figure 7). The N_{total} content shows no clear trend, except a slight decrease, from 1900 to 2000 AD where it varies from 0.34 to 0.29%. As a result, the C/N ratio increases between the bottom and the top of the core.

The $\delta^{15}N$ shows variations bracketed by values of 8.52 to 9.66 ‰, with a minimum between 1700 and 1800 AD. The $\delta^{13}C$ signature shows a slight decrease from -22.90 to -22.48 ‰.

3.2. PALYNOLOGY

Dinocysts are the most abundant palynomorphs throughout the core in addition to pollen, spores, organic linings of foraminifers, thecamoebians and acritarchs. Dinocyst concentrations vary between 2500 and 5000 dinocysts g^{-1} dry sediment in the lower part of the core, between 1560 and 1820 AD (46-19 cm) (Figure 8, Annexe II, Table 4). Their concentrations reach maximum values of about 13,000 dinocysts g^{-1} between 1820 and 1920 AD (19-11 cm). Considering the sedimentation rate of 0.10 cm yr^{-1}, these concentrations correspond to mean flux of about 6600 dinocysts cm^{-2} yr^{-1} and allows comparison with those measured by Hamel *et al.* (2002) in the same region. Such fluxes are very high compare to other subpolar settings and reflect high primary productivity (Rochon et de Vernal, 1994). Hamel *et al.* (2002) observed similar fluxes and they seem to be

characteristic of the high productivity of the North Water Polynya. The low and constant values (<0.2) of the Gonyaulacales/Peridiniales ratio (G/P) indicate that the dinocyst assemblages are mostly dominated by heterotrophic taxa throughout the core and that autotrophic taxa are mostly accompanying taxa with the exception of the Gonyaulacales *Operculodinium centrocarpum* s.l. which includes *Operculodinium centrocarpum* and the variations "short spines" and "arctic". Similar observations were made by Hamel *et al.* (2002).
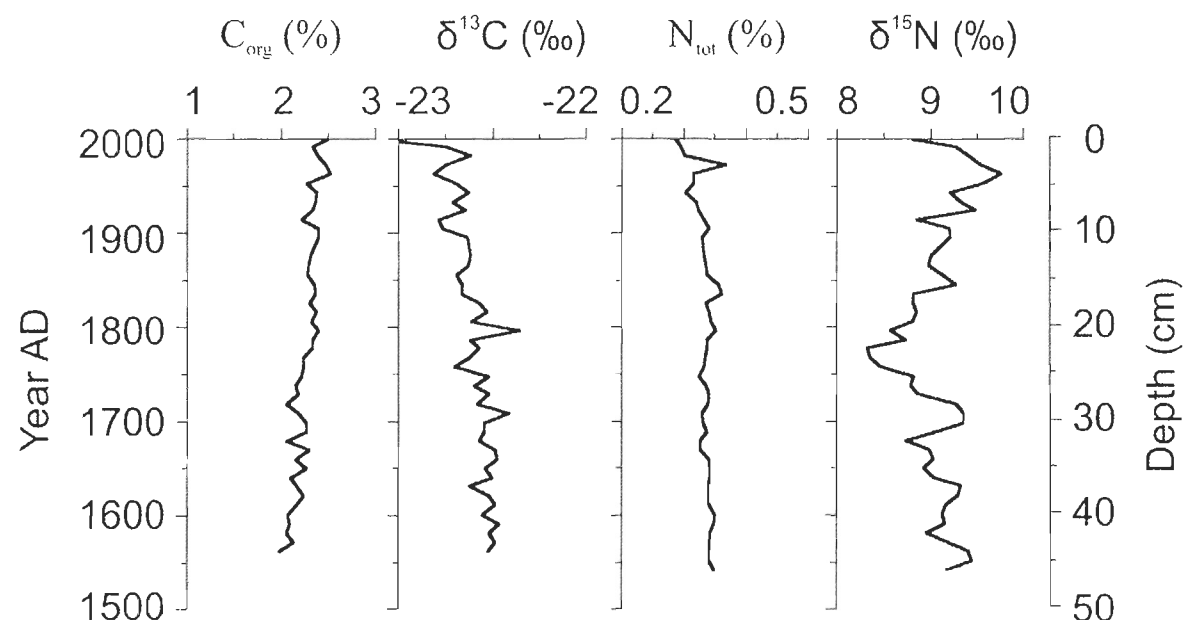
Figure 7. Carbon and nitrogen content of the sediments core 2008-029-040 BC-C. The age model data are presented in Figure 2.
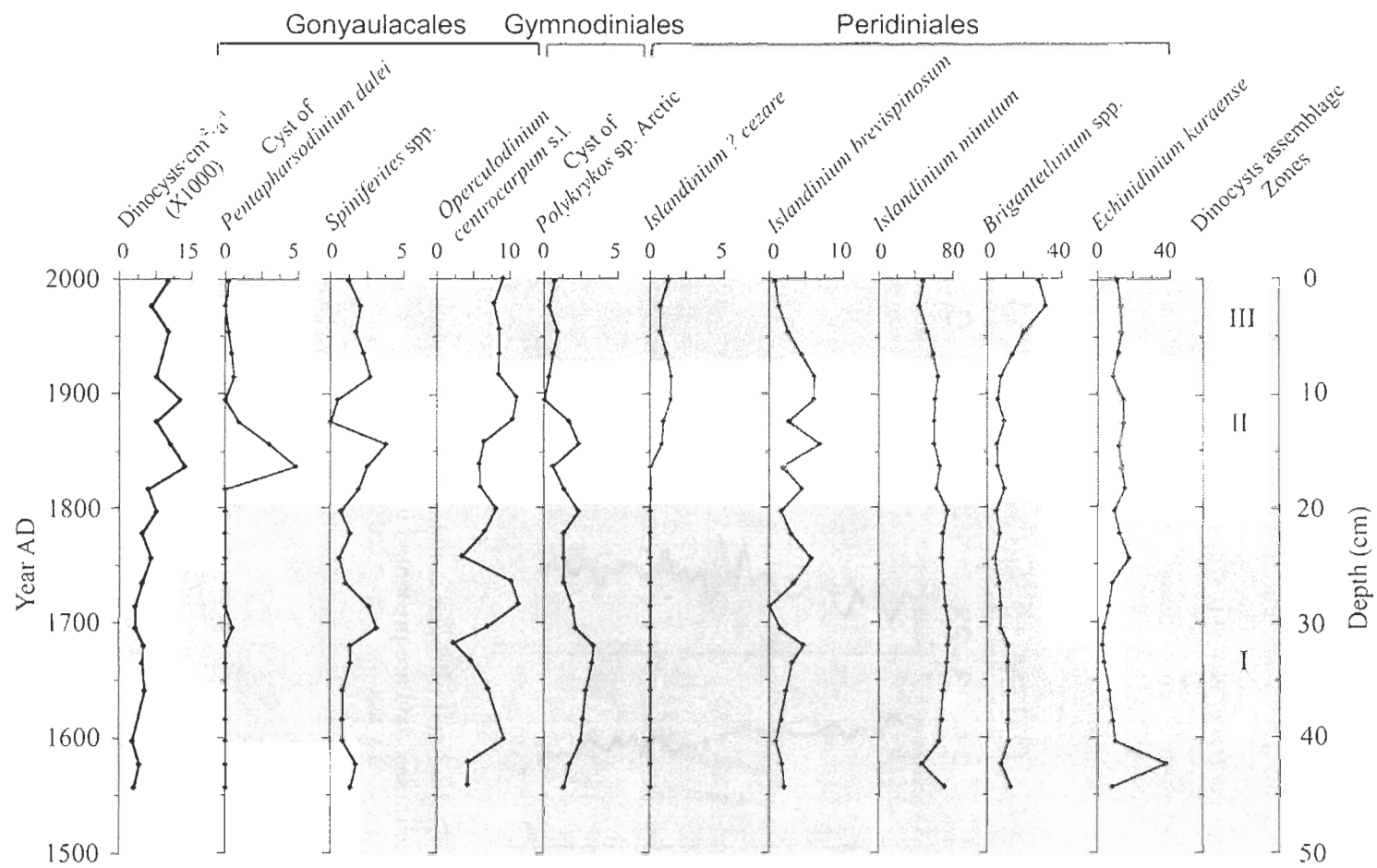
Figure 8. Dinocyst fluxes, Gonyaulacales vs. Peridiniales ratio (G/P) and relative abundance of dinocyst taxa from the Gonyaulacales (in green), Gymnodiniales (in brown) and Peridiniales (in orange) in core 2008-029-040 BC. *Spiniferites* spp. includes *Spiniferites elongatus* and *S. frigidus*, *Operculodinium centrocarpum* s.l. includes *Operculodinium centrocarpum* and the 'short spines' and 'arctic' morphotypes. Note the various scales for the *x*-axis. Dinocyst assemblage zones were determined using XLSTAT 2012 software by a hierarchical clustering of samples (See dendogram dissimilarities Figure 12).

Statistical analyses by a hierarchical clustering of samples allowed distinguishing three different dinocyst assemblage zones based on their relative abundance (see dendogram dissimilarites in Annexe III, Figure 12). Dinocyst assemblage zone I (Figure 8), between 1560 and 1800 AD (46-20 cm), is characterised by the maximum abundance of *Islandinium minutum* with a mean value of 71 % accompanied by *Brigantedinium* spp., *Operculodinium centrocarpum* s.l. and *Echinidinium karaense*. This zone is also characterized by the occurrence of the following accompanying taxa: *Ataxiodinium choane* (not illustrated), *Impagidinium aculeatum* (not illustrated), cyst of *Pentapharsodinium dalei*, *Spiniferites* spp., cyst of *Polykrikos* sp. Arctic and *Islandinium brevispinosum*. Dinocyst assemblage zone II, between 1800 and 1935 AD (20-7 cm), is characterised by the highest dinocyst fluxes and occurrence of accompanying taxa (e.g. *Impagidinium aculeatum* (not illustrated), cyst of *Pentapharsodinium dalei* and *Spiniferites* spp., *Islandinium*? cezare), while *Islandinium minutum* and *Echinidinium karaense* still dominate the assemblages. Finally, dinocyst assemblage zone III, between 1935 and 2000 AD (7-0 cm), is characterised by the highest occurrence of *Brigantedinium* spp. and *Operculodinium centrocarpum* s.l., and by the lowest occurrence of *Islandinium minutum* and *Islandinium brevispinosum*.

3.3. RECONSTRUCTION OF PAST SEA-SURFACE CONDITIONS

Reconstructed sea-surface conditions also show significant variations since 1560 AD (cm 46). In dinocyst assemblage zone I, between 1560 and 1800 AD (46-20 cm), the mean SST_a is 1.8 ± 0.3 °C while dinocyst assemblage zones II and III led to reconstruct mean SST_a of 2.5 ± 0.4 and 2.1 ± 0.1 °C, respectively (p-value = 0.01) (Figure 9). Similarly, the mean reconstructed SIC is 9.1 ± 0.2 months yr^{-1} in assemblage zone I while the mean reconstructed SIC in assemblage zones II and III decrease to 8.1 ± 0.6 and 8.3 ± 0.1 months yr^{-1}, respectively (p-value = 0.0001). Finally, mean reconstructed APP show relatively low annual values. This is not surprising as they represent only 2 to 3 months of primary productivity when surface waters are free of ice. Mean reconstructed APP was of 92 ± 5 gC

cm^{-2} yr^{-1} in zone I, while zones II and III show an mean reconstructed APP of 105 ± 9 and 111 ± 3 gC cm^{-2} yr^{-1}, respectively (p-value = 0.001).

A peak of APP is observed in assemblage zones I and II (Figure 9, peaks A and B respectively). Peak A is in sediments accumulated between 1690 and 1740 AD (33-28 cm). In this zone, the reconstructed APP and SST_a increase from 85 to 115 gC cm^{-2} yr^{-1} and from 1.58 to 2.58 °C, respectively, while the reconstructed SIC remains constant at ~ 9 months yr^{-1}. Peak B is in sediments accumulated between 1880 and 1915 AD (13-10 cm). In this zone, the reconstructed APP increases from 95 to 124 gC cm^{-2} yr^{-1}. Also, the dinocyst assemblage in this zone suggests an increase of the SSTa from 1.87 to 3.43 °C and a decrease of the SIC from 9 to 7 months yr^{-1}.

3.4. ORGANIC BIOMARKERS

Nearly all of the analysed organic biomarkers (straight chain alkanes, pristane and phytane, sterols, and IP_{25}) follow the same trend as the reconstructed APP (Figure 9 and Table 5). Figure 10 shows a typical partial GC chromatogram of the sterol fractions in which the main analysed compounds are identified. Moreover, we built a Pearson Correlation Matrix to assess the relationships between the main studied variables and organic biomarkers (Table 2). The stronger correlation coefficient (R^2=0.72) involving an organic biomarker is between IP_{25} and reconstructed APP, similar to the one between reconstructed SSTa and reconstructed APP (R^2=0.76) (Table 2), a known relationship. In fact, the rate of photosynthesis is strongly temperature-dependant (Hikosaka et al., 2006). This also suggests an important relationship between APP and IP_{25} concentration.
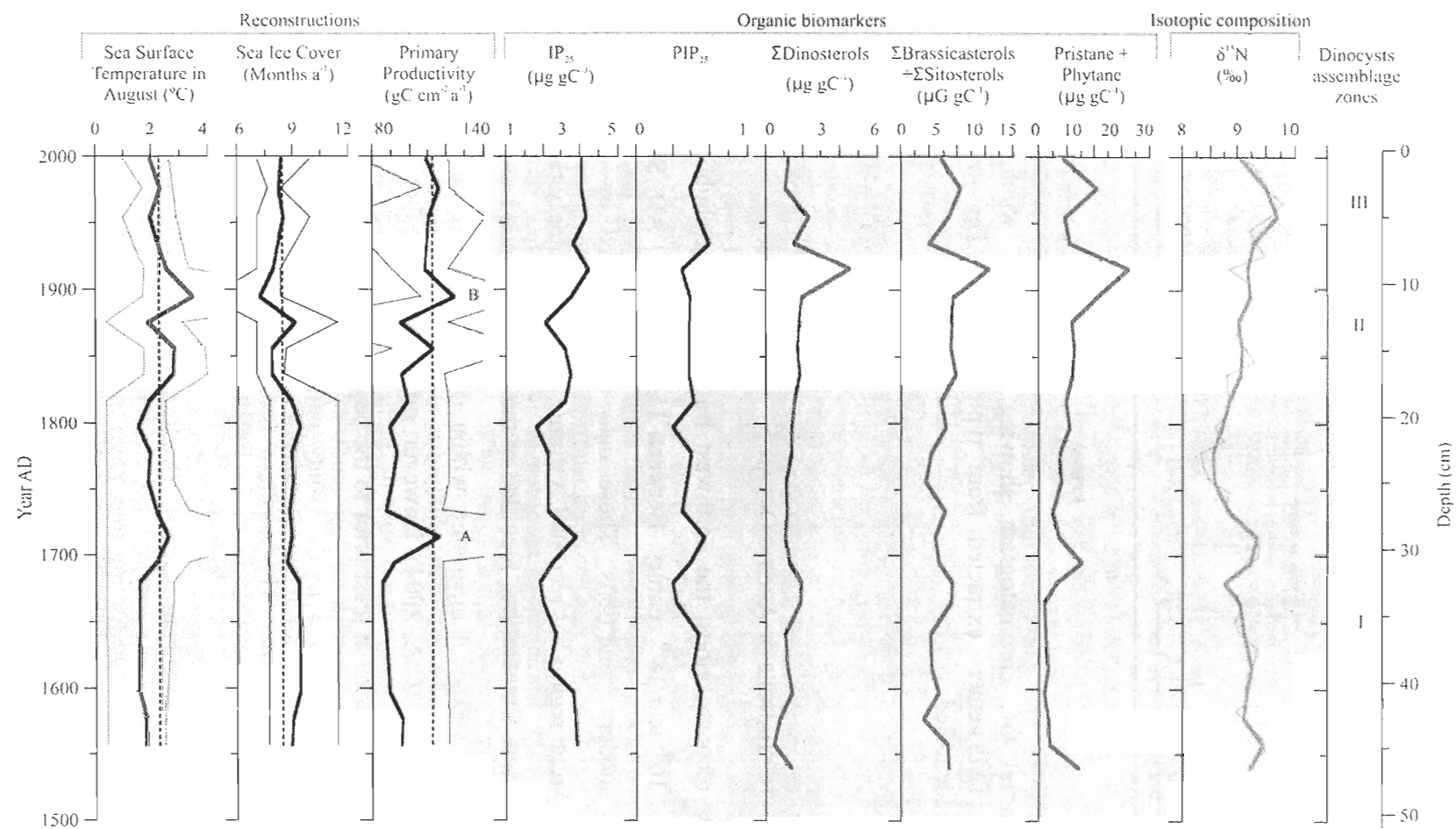
Figure 9. Quantitative estimates of sea-surface conditions based on the Modern Analogue Technique, isotopic composition ($\delta^{15}N$) of organic matter and major organic biomarkers in core 2008-029-040 BC. For the reconstructions, the thick lines correspond to the best estimates and the thin lines correspond to the minimum and maximum possible values according to the set of analogues. The vertical dashed lines correspond to the modern values for each parameter. For the isotopic composition, the thin lines represent the actual data and the thick lines represent smoothed values averaged over 4 data points.
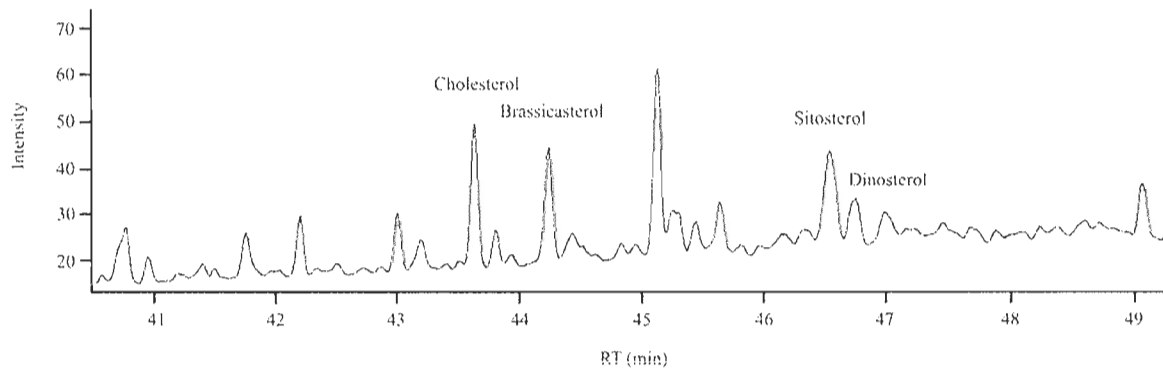
Figure 10. Partial GC chromatogram showing the elution window for sterol trimethylsulyl (TMS)-ethers extracted from typical sample. The main discussed compounds are identified.

4. DISCUSSION

4.1. RECENT CLIMATE CHANGES OF ARCTIC OCEAN

Based on our reconstructions, the northwest Baffin Bay was slightly cooler than present between the 16th and 18th century. Between 1560 and 1800 AD, SST was about 0.6°C cooler than modern conditions. These data are supported by others studies confirming that the Arctic region has recorded warming at an increasingly rapid pace since the 1900s. While average temperatures recorded at the Earth's surface have increased by 0.74°C since 1906, the average temperature within the Arctic circle has increased by 0.90°C from 1900 to 2002 (ACIA, 2004). However, our results show that in the northern Baffin Bay, this warming started at least prior to the beginning of the industrial era around 1800 AD. Such warming observed in this study could be explained by a change in atmospheric or oceanic circulation. The northern Baffin Bay circulation (Figure 4) is dominated by a strong, cold southward flow, the Baffin Current, and a weaker but warmer northward flow, the West Greenland Current (Melling et al., 2001). Moreover, several studies have suggested that ocean forcing may exert an important control on modern ice sheet dynamics and other oceanographic parameters by the influence of warmer ocean

conditions (Joughin *et al.*, 2004; Thomas, 2004; Bindschadler, 2006; Holland *et al.*, 2008). The water mass properties of the Baffin Current and the West Greenland Current are linked to the large-scale Arctic and North Atlantic climate system, respectively (e.g. Perner *et al.*, 2012). Thus, shifts in the relative contribution of the relatively cold/strong Arctic (Baffin Current) and warmer/weak Atlantic (West Greenland Current) water masses to the northern Baffin Bay could explain the slight warming observed and the increased occurrence of autotrophic taxa (e.g. cyst of *Pentapharsodinium dalei*, *Operculodinium centrocarpum* s.l. and *Spiniferites* spp.). Hamel *et al.* (2002) proposed that the conditions in northern Baffin Bay are more favorable for the growth of autotrophic dinoflagellates than in the North Water because of lesser diatom productivity and competition than in the highly productive upwelling area.

The positive phase of the Arctic Oscillation (AO) and the Pacific North American (PNA) circulation index seem to influence positive Surface Air Temperature (SAT) anomalies mostly over the continental areas of the Arctic during the major part of the 20th century. Even the beginning of the 21st century shows positive Arctic-wide SAT anomalies consistent with IPCC-AR4 model projections based on anthropogenic forcing (Overland *et al.*, 2008; Stroeve *et al.*, 2011). Consequently, this atmospheric pattern could also explain in part the slight warming in the 19th-20th century observed in the northern Baffin Bay.

In conjunction with this warming, our reconstructions also show a decrease of the SIC during the 19th and early 20th centuries, this following the trend observed throughout the Arctic in the recent years (Rigor et Wallace, 2004; Stroeve *et al.*, 2011). However, the minimum and maximum probable values in our reconstructed SIC suggest that these variations are not significant. Nonetheless, in the dinocyst assemblage zone I, between 1560 and 1800 AD, the mean reconstructed SIC is about one month higher than modern values.

Table 2. Pearson Correlation Matrix for the main studied variables. The values were determined using XLSTAT 2012 software.

Variables	G/P	Dinocysts cm^{-2} yr^{-1}	SST$_a$	SIP	APP	C$_{org}$	δ^{13}C	N$_{total}$	δ^{15}N	C/N	IP$_{25}$	PIP$_{25}$	Σdinosterols	$\Sigma(\Sigma$brassicosterols+Σsitosterols)	Pristane & phytane
G/P	1.00	0.45	**0.73**	**-0.62**	0.57	0.37	-0.21	0.05	0.23	0.26	0.45	0.33	0.19	0.14	0.41
Dinocysts cm^{-2} yr^{-1}	0.45	1.00	**0.62**	**-0.78**	0.52	**0.66**	**-0.61**	-0.13	0.10	0.56	0.32	-0.04	0.36	0.37	0.45
SST$_a$	**0.73**	**0.62**	1.00	**-0.90**	**0.76**	0.37	-0.37	0.04	0.26	0.24	0.43	0.13	0.27	0.36	**0.62**
SIP	**-0.62**	**-0.78**	**-0.90**	1.00	**-0.77**	-0.50	**0.67**	0.16	-0.33	-0.45	-0.56	-0.11	-0.39	-0.53	**-0.73**
APP	0.57	0.52	**0.76**	**-0.77**	1.00	0.43	-0.58	-0.35	0.54	0.50	**0.72**	0.41	0.20	0.32	**0.60**
C$_{org}$	0.37	**0.66**	0.37	-0.50	0.43	1.00	-0.35	-0.26	-0.06	**0.87**	0.13	-0.03	0.30	0.17	0.50
δ^{13}C	-0.21	**-0.61**	-0.37	0.67	-0.58	-0.35	1.00	**0.66**	-0.37	**-0.61**	**-0.67**	-0.32	-0.23	-0.35	-0.41
N$_{total}$	0.05	-0.13	0.04	0.16	-0.35	-0.26	**0.66**	1.00	-0.19	**-0.70**	-0.32	-0.21	-0.15	-0.06	-0.11
δ^{15}N	0.23	0.10	0.26	-0.33	0.54	-0.06	-0.37	-0.19	1.00	0.06	**0.75**	0.50	0.01	0.22	0.23
C/N	0.26	0.56	0.24	-0.45	0.50	**0.87**	**-0.61**	**-0.70**	0.06	1.00	0.27	0.11	0.28	0.14	0.41
IP$_{25}$	0.45	0.32	0.43	-0.56	**0.72**	0.13	**-0.67**	-0.32	**0.75**	0.27	1.00	**0.65**	0.25	0.38	0.44
PIP$_{25}$	0.33	-0.04	0.13	-0.11	0.41	-0.03	-0.32	-0.21	0.50	0.11	**0.65**	1.00	-0.34	-0.45	-0.17
Σdinosterols	0.19	0.36	0.27	-0.39	0.20	0.30	-0.23	-0.15	0.01	0.28	0.25	-0.34	1.00	**0.78**	**0.66**
$\Sigma(\Sigma$brassicosterols+Σsitosterols)	0.14	0.37	0.36	-0.53	0.32	0.17	-0.35	-0.06	0.22	0.14	0.38	-0.45	**0.78**	1.00	**0.77**
Pristane & phytane	0.41	0.45	**0.62**	**-0.73**	**0.60**	0.50	-0.41	-0.11	0.23	0.41	0.44	-0.17	**0.66**	**0.77**	1.00

Finally, the reconstruction based on dinocyst assemblages suggest that the decreasing SIC and the increasing SST_a are accompanied by an increase of the annual pelagic primary productivity in northern Baffin Bay by about 16 % during the 19th and early 20th centuries. Primary productivity could be enhanced directly by increasing sea surface temperature, but also indirectly through reduction of the ice cover thickness, allowing light penetration in the upper water column. However, it was shown that marine primary productivity is enhanced at the ice-edge due to a stabilisation of the water column and increased nutrient release from melting sea ice (Smith Jr *et al.*, 1987; Sakshaug, 2004; Wassmann, 2004). The oceanographic changes observed in this work might have resulted in more favourable conditions for phytoplankton linked to more stable ice-edge conditions.

4.2. NORTH WATER POLYNYA INPUT

According to Meyers (1997), the relatively low $\delta^{13}C_{org}$ values of the sediments reflect the predominantly marine origin of the organic matter fluxes over terrestrial inputs (Figure 11). These values are similar to those of the modern North Water plankton (Tremblay *et al.*, 2006) and dissolved organic matter (DOM) of the North Atlantic (James *et al.*, 2002). Elsewhere in Arctic sediments, similar values of $\delta^{13}C_{org}$ have also been interpreted as reflecting the marine character of the organic matter fluxes during the late Holocene in the Chukchi Sea (McKay *et al.*, 2008), Laptev Sea (Mueller-Lupp *et al.*, 2000), Kara Sea (Kang *et al.*, 2007; Nagel *et al.*, 2009) and in the Canadian Arctic Archipelago (Ledu *et al.*, 2008). Moreover, these low $\delta^{13}C_{org}$ values are in agreement with the low lipid ratios between long (carbon number $\geq$ 25) and short ($\leq$ 24) straight-chain n-alkanes from our record.
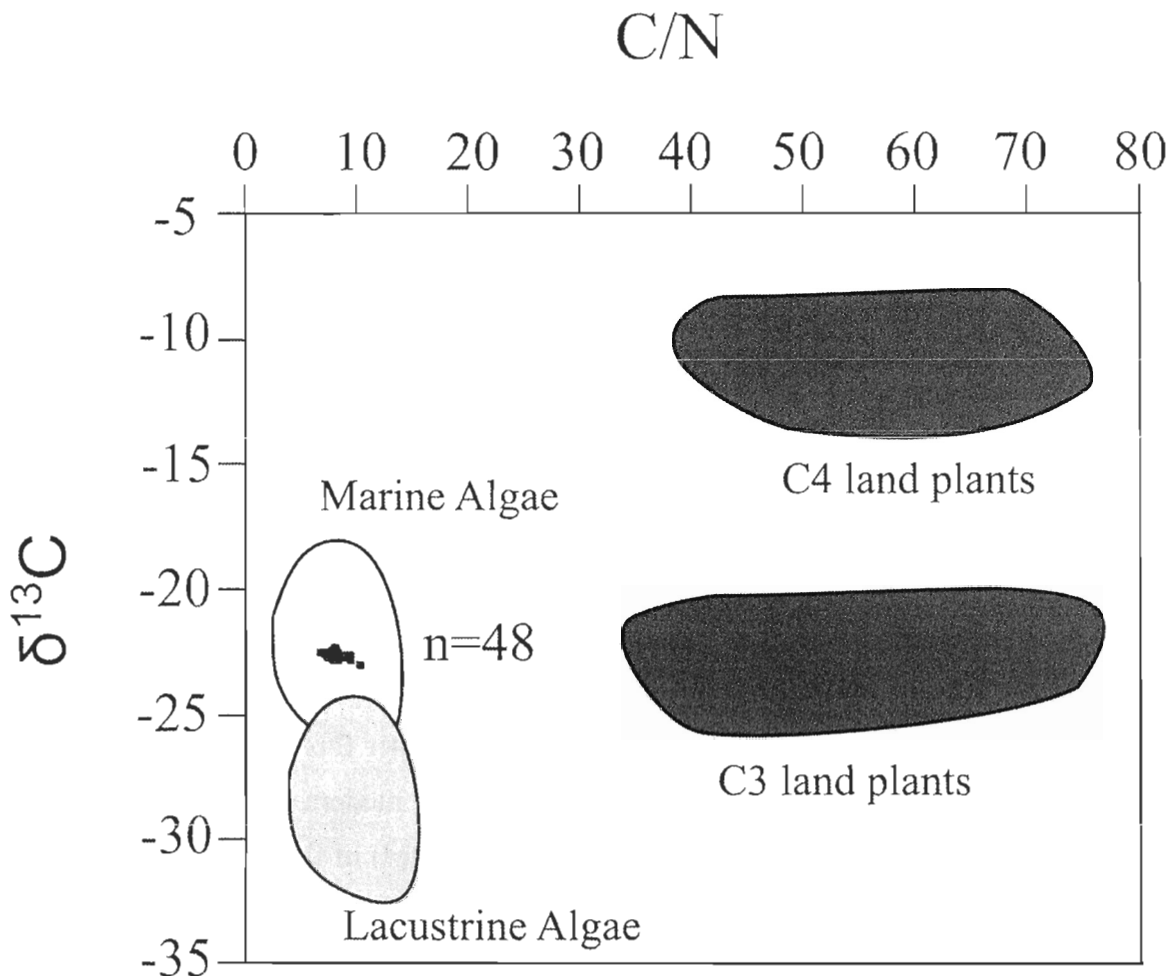
Figure 11. Elemental (atomic C/N ratio) and isotopic (δ^{13}C value) identifiers of bulk organic matter produced by marine algae, C_3 land plants, and C_4 land plants. The blue squares represent data from core 2008-029-040 BC. Adapted from Meyers (1997).

Several indicators using straight-chain n-alkanes have been developed to estimate the relative contribution between terrigenous and marine organic matter to the sediments (Hautevelle *et al.*, 2007; Xu et Jaffé, 2007). We use the proxy developed by Hautevelle et al (2007) because it includes more lipids values, although all tested proxies gave similar results (Table 5). This proxy is illustrated as:

$$n-C_{24}^+/n-C_{24}^- = \sum n-C_i/\sum n-C_j$$

$$i = 25 - 34 \quad j = 17 - 24$$

Typically, long (25-36 carbon atoms) straight-chain n-alkanes ($\sum n - C_i$) are used as terrigenous biomarkers (Eglinton et Eglinton, 2008) while phytoplankton is estimated to be the main source of the short (e.g. C_{17}, C_{19}, C_{21}) straight-chain n-alkanes ($\sum n - C_j$) (Blumer *et al.*, 1970; Blumer *et al.*, 1971; Rosell-Melé et McClymont, 2007; Burns *et al.*, 2008). Consequently, the low measured values (mean = 0.68) of $n-C_{24}^+/n - C_{24}^-$ should also reflect the predominantly marine origin of the organic matter fluxes.

The C:N atomic ratio can also been used as a tracer for the origin of organic matter. The C:N ratio is generally high in terrigenous DOM and low in marine DOM (Meyers, 1997; Dennis et Craig, 2002). A mean C:N ratio of 20.5 was reported for seven Siberian rivers (Gordeev *et al.*, 1996). For example, the C:N ratios of the Beaufort Sea sediments, strongly influenced by the Mackenzie River, could go up to 16.0 (Drenzek *et al.*, 2007). The low C:N ratios (mean = 7.87) measured in our sediments also suggest a predominantly marine origin of the organic matter fluxes.

The relatively high $\delta^{15}N$ values measured in the sediments, particularly in the two peaks of APP (Figure 9, peaks A and B), support this hypothesis and may reflect stronger nitrogen recycling during warmer periods as low $\delta^{15}N$ values reflect algal discrimination in favour of ^{14}N. Low $\delta^{15}N$ values might record periods of enhanced nitrate availability, while high $\delta^{15}N$ reflect more oligotrophic conditions (Calvert *et al.*, 1992; Meyers, 1997). The correlation between $\delta^{15}N$ values and the reconstructed annual primary productivity (R^2=0.54, Table 2) suggests that the nitrogen could have been and could become a limiting factor for algal growth in a warmer Arctic Ocean. However, it also suggests that the input of nitrogen were not responsible for the recent primary productivity increases, but more likely the result of an increase of SST and reduction of SIC.

4.3. PRIMARY PRODUCTIVITY

Our biomarkers results suggest that the dinoflagellates are not the main contributors to the primary productivity. There is only a weak relationship between dinocyst fluxes and

APP (R^2=0.52; Table 2) and the peak A precedes the maximum dinocyst influx (zone II) (Figure 9, peaks A and Table 2). Moreover, the low and relatively constant values of the G/P ratio indicate that the dinocyst assemblages are dominated by heterotrophic taxa, which graze mainly on primary producers such as diatoms. As suggested by Hamel *et al.* (2002), the dominance of heterotrophic taxa in the North Water Polynya can be explained by a high abundance of suitable pelagic prey, mostly diatoms (Booth *et al.*, 2002), which are the main food source for heterotrophic dinoflagellates and may compete the nutrients to the autotrophic dinoflagellates (Dale, 1996; Saetre *et al.*, 1997). This hypothesis is further supported by the work of Mostajir *et al.* (2001), who measured a higher abundance of diatoms in the North Water Polynya than in northern Baffin Bay during the fall season.

In assemblage zone I, and more particularly in the peak A of APP (between 1690 and 1740 AD), while the concentration of many alkanes and sterols covary with primary productivity, the concentration of Σdinosterols is relatively low and invariant (Figure 9, peak A). Dinosterols are known to be good qualitative proxies of the contribution of dinoflagellates to organic carbon deposits (Mouradian *et al.*, 2007). However, other studies have reported that these 'dinoflagellate' molecules could also be produced by other organisms, such as diatoms (Versteegh et Blokker, 2004; Giner et Wikfors, 2011). The low concentrations of the dinosterols in sediments represent nonetheless a weak contribution of dinoflagellates to the primary productivity at the time of deposition.

Brassicasterol (Marty *et al.*, 2008) and sitosterol (Volkman *et al.*, 1993; Volkman, 2003; Mejanelle et Dachs, 2009) are almost exclusively produced by haptophytes. In addition, brassicasterol often account for 90% of sterols in some diatoms species from highly productive areas (Lasternas *et al.*, 2008). Nevertheless, brassicasterol may also represent up to 53% of total sterols in certain dinoflagellate species (Conte *et al.*, 2004) and sitosterol may also be an important component of dinoflagellate sterols (Volkman *et al.*, 1993). Considering the relatively low concentration of dinosterol in assemblage zone I, and particularly in the peak A, it is assumed that the dinoflagellate contribution to the brassicasterols and sitosterols is minimal.

The good relationship between reconstructed APP and IP_{25} (R^2=0.72) compared to Σsitosterol and Σbrassicasterol (R^2=0.40) and Σdinosterol (R^2=0.20) (Table 2) may be related to the fact that diatoms are the major contributors to the primary productivity. These results are consistent with modern North Water Polynya conditions in which diatoms are mostly responsible to the seasonal changes in phytoplankton biomass (e.g. Mei *et al.*, 2005). Similarly to other C_{25} and C_{30} highly branched isoprenoid (HBI) alkenes (Volkman *et al.*, 1994; Damste *et al.*, 2004; Massé *et al.*, 2004), IP_{25} seems to be biosynthesised by a limited number of diatom genera. More specifically, it is likely that IP_{25} is produced by the genus *Haslea* but no study has shown this definitively. However, IP_{25} has only been found in seasonal sea ice environment (Belt *et al.*, 2007). Consequently, the stronger correlation between IP_{25} concentration and primary productivity suggests that it is diatoms living in proximity to sea-ice that account for the increase of primary productivity observed throughout the core. Furthermore, in our sediment core, both IP_{25} and general phytoplankton biomarkers concentration (e.g. brassicasterol, sitosterol, and short chain n-alkanes) suggest favourable conditions for both ice algae and open-water phytoplankton induced by possible stable ice-edge conditions. Such sea-ice conditions are consistent with the reconstructed SIC (mean = 9 months yr^{-1}) and a moderate PIP_{25} index, which has been defined as a corrected ratio between IP_{25} and general phytoplankton biomarkers (Muller *et al.*, 2011).

$$PIP_{25} = IP_{25}/\left(IP_{25} + (phytoplankton\ marker\ \times c)\right)$$

$$c = mean\ IP_{25}/mean\ phytoplankton\ biomarker\ concentration$$

A high PIP_{25} index reflects lasting ice cover conditions, where ice algae inhabiting sea ice could grow freely, as opposed to other types of phytoplankton, which are limited by low light conditions. However, a low PIP_{25} index reflects predominantly ice-free conditions where general phytoplankton could grow freely, whereas the growing ice algae are limited by low sea-ice concentrations (Muller *et al.*, 2011). For example, in the peak A (between 1690 and 1740 AD) in the dinocyst assemblage zone I and in the dinocyst assemblage zone II (Figure 9), the IP_{25} concentration increases by 48%, while general phytoplankton

biomarkers remain relatively constant. This situation results in a more elevated PIP_{25} index (0.61) and correspond to conditions more favorable to sea-ice diatoms in this zone. However, in the remainder of the core, the PIP_{25} index remains relatively low and constant (0.49), suggesting favourable living conditions for both ice algae and open-water phytoplankton (Figure 9).

The reconstruction of sea-surface parameters show a small decrease of the SIC during the 19th and early 20th centuries. These reconstructions are consistent with the trend observed throughout the Arctic and they are strongly supported by the results obtained for others proxies. For example, the higher temperatures are supported by lower sea-ice presence (passing from a higher sea-ice context to a more stable ice edge context) and by stronger primary productivity. However, the IP_{25} concentrations are correlated to primary productivity proxies (e.g. brassicasterol, $\delta^{15}N$, reconstructed primary productivity) rather than reconstructed SIC, which suggests that the production of IP_{25} can be influenced by the same factors influencing the production of other primary productivity proxies, such as the availability of nutrients, SST, irradiance and brines within the sea-ice. The relationship between ice cover and primary productivity is not a simple inverse one. The primary productivity is affected by different sea-ice scenarios and in that case, IP_{25} helps to distinct the evolution from a higher sea-ice context to a more stable ice edge context. The IP_{25} is no doubt related to the presence of sea ice over multi-centennial timescales (Axford *et al.*, 2011; Muller *et al.*, 2011), but our results show that IP_{25} is probably less sensitive than dinocyst assemblages to trace quantitatively the sea-ice cover fluctuations. Accordingly, IP_{25} could be useful to evaluate the primary productivity in association with the sea-ice in seasonal sea-ice environments rather than the fluctuation of the sea-ice cover concentration.

5. CONCLUSION

Our multi-proxy study of a northern Baffin Bay sediment record allows comparing two sea-ice proxies over the last 500 years, IP_{25} and MAT using dinoflagellate cyst assemblages. Our study was unable to establish a link, through comparison of proxies,

between the amount of IP_{25} in sediments and the sea-ice cover. Our results show that IP_{25} is sensitive to the primary productivity in association with the sea-ice but does not unequivocally reflect the fluctuation of the sea-ice concentrations.

Our results also show that the 19th and early 20th centuries were slightly warmer than 16th, 17th and 18th centuries in northwest Baffin Bay. Since 1800 AD, SST increased by about 0.6°C compared with the previous three centuries, which coincides with a decrease of the SIC and an increase of the pelagic annual primary productivity in northern Baffin Bay. Such a change in surface conditions could be related to a greater contribution of the warmer West Greenland current, which would also explain the increased occurrence of autotrophic dinoflagellate taxa.

Finally our primary productivity data suggest an ecosystem dominated by diatoms in interaction with the sea-ice, where the sea-ice conditions would be the main limiting factors for primary productivity and where nutrients could eventually become limiting in a warmer Arctic.

CONCLUSION

Notre étude multi-traceurs dans le nord de la baie de Baffin a permis de comparer sur les 500 dernières années, deux traceurs de glace, l'IP_{25} et la méthode des analogues modernes appliquée aux kystes de dinoflagellés.

Notre étude n'a pu établir de lien, sur la base de cette comparaison, entre les quantités d'IP_{25} retrouvées dans les sédiments et les concentrations de glace de mer. Nos résultats suggèrent que l'IP_{25} est donc moins sensible que les assemblages de dinokystes pour retracer les fluctuations de la glace de mer. Toutefois, IP_{25} pourrait s'avérer utile pour évaluer la productivité primaire en association avec la glace de mer plutôt que pour évaluer les fluctuations de la concentration de glace de mer elle-même.

Des études approfondies sur les mécanismes et les processus responsables de la production ou influençant la production, la conservation et la sédimentation des biomarqueurs organiques permettraient une utilisation plus efficace des biomarqueurs. Par ailleurs, malgré l'utilisation de biomarqueurs organiques de plus en plus spécifiques, leur source peut avoir diverses origines et être difficile à déterminer. L'analyse de la composition isotopique des biomarqueurs permettrait une meilleure évaluation de leurs origines tout en fournissant des informations environnementales supplémentaires.

En combinant l'analyse des assemblages de dinokystes, des biomarqueurs organiques, ainsi que de la composition isotopique de l'azote ($\delta^{15}N$) et du carbone

organique ($\delta^{13}C_{org}$) dans une séquence sédimentaire du nord de la baie de Baffin, notre étude montre aussi que dans la région, les conditions de surface des 16ème, 17ème et 18ème siècles ont été légèrement plus fraiches que celles du 19ème et du début du 20ème siècle. Depuis 1800 AD, la température marine de surface a augmenté d'environ 0,6° C par rapport aux trois siècles précédents. En parallèle à ce réchauffement, nos reconstitutions quantitatives des conditions marines de surface montrent une diminution de la concentration de glace de mer. Enfin, nos reconstitutions suggèrent que la diminution de la glace de mer ainsi que l'augmentation de la température ont été accompagnées d'une augmentation de la productivité primaire pélagique annuelle. Comme ce réchauffement semble avoir été initié au tout début de l'ère industrielle, vers 1800 AD, il peut difficilement être expliqué par les activités humaines. Une explication alternative probable serait une influence croissante dans la région du courant plus chaud de l'ouest du Groenland plutôt que par le forçage anthropogénique. D'ailleurs, l'influence plus grande de ce courant pourrait expliquer l'augmentation de taxons autotrophes de dinoflagellés.

Nos résultats pour les indicateurs organiques de productivité pélagique primaire suggèrent un écosystème dominé par les diatomées en interaction avec la glace de mer, où la température de surface marine et les conditions de glace de mer seraient les principaux facteurs limitant la productivité primaire et où les nutriments pourraient devenir limitant dans un Arctique encore plus chaud.

Quoi qu'il en soit, une étude plus approfondie sur des échelles de temps géologiques et surtout, illustrant l'évolution d'un système changeant, permettrait une meilleure évaluation de la portée des différents traceurs utilisés dans cette étude.

Table 3. Excel spreadsheet calculations of estimated age vs. depth in box core 2008-029-040 BC based on CRS model

Depth midpoint	Depth (1)	Depth (2)	Water quantity	Porosity (φ)	Masse volumique (d)	Sediment weight	Cumulative mass depth	Midpoint mass depth	^{210}Pb	$\pm$	$^{210}Pb_{exs}$	In $^{210}Pb_{exs}$	^{226}Ra	$\pm$	Slice Inventory	Cummulative Inventory	Cum-Slice Inventory	Sedimentation rate	Age ^{210}Pb (CRS)
	cm		%		g cm⁻³		g cm⁻²					dpm g⁻¹						g cm⁻² yr⁻¹	yr
0.5	0	1	78.20	0.90	0.25	0.25	0.25	0.13	10.0	0.8	7.2	2.0	2.80	0.09	1.8	1.8	18.8	0.2	3.0
1.0	0	2																	
1.5	1	2	75.28	0.89	0.29	0.29	0.54	0.40	10.0	0.8	7.1	2.0	2.85	0.07	2.1	3.9	16.7	0.2	6.7
2.0	1	3																	
2.5	2	3	70.00	0.86	0.37	0.37	0.91	0.73	10.3	0.8	7.5	2.0	2.78	0.07	2.7	6.6	14.0	0.2	12.5
3.0	2	4																	
3.5	3	4	66.46	0.83	0.42	0.42	1.33	1.12	9.2	0.7	6.5	1.9	2.70	0.07	2.7	9.4	11.3	0.2	19.5
4.0	3	5																	
4.5	4	5	62.33	0.81	0.49	0.49	1.82	1.57	9.7	0.7	7.1	2.0	2.65	0.07	3.5	12.8	7.8	0.1	31.3
5.0	4	6																	
5.5	5	6	67.38	0.84	0.41	0.41	2.23	2.02	8.7	0.7	6.0	1.8	2.70	0.09	2.4	15.3	5.4	0.1	43.3
6.0	5	7																	
6.5	6	7	72.67	0.87	0.33	0.33	2.55	2.39	6.3	0.5	3.6	1.3	2.73	0.09	1.2	16.4	4.2	0.1	51.3
7.0	6	8																	
7.5	7	8	58.79	0.78	0.55	0.55	3.10	2.83	5.7	0.4	2.8	1.0	2.82	0.10	1.6	18.0	2.6	0.1	66.3
8.0	7	9																	
8.5	8	9	63.25	0.81	0.47	0.47	3.58	3.34	5.7	0.4	3.2	1.1	2.58	0.06	1.5	19.5	1.1	0.1	93.4
9.0	8	10																	
9.5	9	10	57.44	0.77	0.57	0.57	4.15	3.86	4.6	0.4	2.0	0.7	2.64	0.10	1.1	20.6	0.0	0.1	
10.0	9	11																	

Total inventory = 20.6333 dpm g⁻¹

ANNEXE II: DINOCYSTS IN BOX CORE HU 2008-029-040 BC-C

Table 4. Count of dinocysts in HU2008-029-040 BC-B

Depth midpoint	Gonyaulacales								
	Ataxiodinium choane	*Impagidinium aculeatum*	*Operculodinium centrocarpum*	*Operculodinium centrocarpum* "short spines"	*Operculodinium centrocarpum* "arctic"	*Spiniferites elongatus*	*Spiniferites frigidus*	*Spiniferites* sp.	Cyst of *Pentapharsodinium dalei*
cm	nb								
0.5	3	0	8	5	13	1	2	0	0
2	0	0	5	2	16	3	3	0	0
4.5	0	0	2	8	15	2	1	0	0
6.5	0	0	25	0	0	7	0	0	1
8.6	0	0	2	3	20	5	1	2	2
10.5	0	3	2	2	29	2	0	0	0
12.5	0	0	0	10	20	0	0	0	3
14.5	0	0	0	2	16	0	11	0	9
16.5	0	0	0	0	17	0	8	0	15
18.5	0	0	0	0	17	0	6	0	0
20.5	0	0	1	0	23	0	2	0	0
22.5	0	0	0	3	16	0	4	0	0
24.5	0	0	0	0	10	0	0	2	0
27	0	0	0	1	29	0	0	3	0
29	0	0	0	0	33	0	0	8	0
31	0	0	0	2	19	0	0	9	2
33	2	0	0	2	4	0	0	4	0
34	2	0	0	2	11	0	0	4	0
36	1	0	0	2	18	0	0	3	0
39	0	0	23	0	0	0	0	2	0
41	0	2	0	2	24	0	0	2	0
43	0	0	0	0	12	0	0	5	0
45	0	0	0	0	12	0	4	0	0

44

Depth midpoint	Gymnodiniales	Peridiniales						
	Cyst of *Polykrikos* sp. "arctic"	*Islandinium minutum*	*Islandinium ?cezare*	*Islandinium brevispinosum*	*Echinidinium karaense*	*Brigantedinium* sp.	*Brigantedinium cariacoense*	*Brigantedinium simplex*
cm	nb	nb						
0.5	2	144	3	2	32	74	2	6
2	1	131	2	4	39	81	4	10
4.5	3	159	2	8	41	52	3	5
6.5	2	176	3	13	33	41	0	0
8.6	1	194	5	18	26	17	0	5
10.5	0	182	4	18	43	14	0	3
12.5	5	179	3	8	44	28	0	0
14.5	7	179	2	20	36	16	0	0
16.5	2	197	0	5	41	17	0	0
18.5	4	188	0	13	45	28	0	0
20.5	7	221	0	5	28	14	0	0
22.5	4	207	0	9	37	20	0	0
24.5	4	205	0	17	52	6	0	6
27	4	210	0	10	24	16	0	3
29	6	215	0	0	17	21	0	0
31	6	228	0	5	9	22	0	0
33	10	224	0	14	8	32	0	2
34	10	220	0	9	10	31	0	2
36	8	208	0	7	19	30	0	4
39	8	201	0	5	49	34	0	0
41	7	195	0	2	29	29	0	5
43	5	139	0	5	113	19	2	0
45	4	213	0	6	24	35	0	2

ANNEXE III: DENDOGRAM DISSIMILARITY
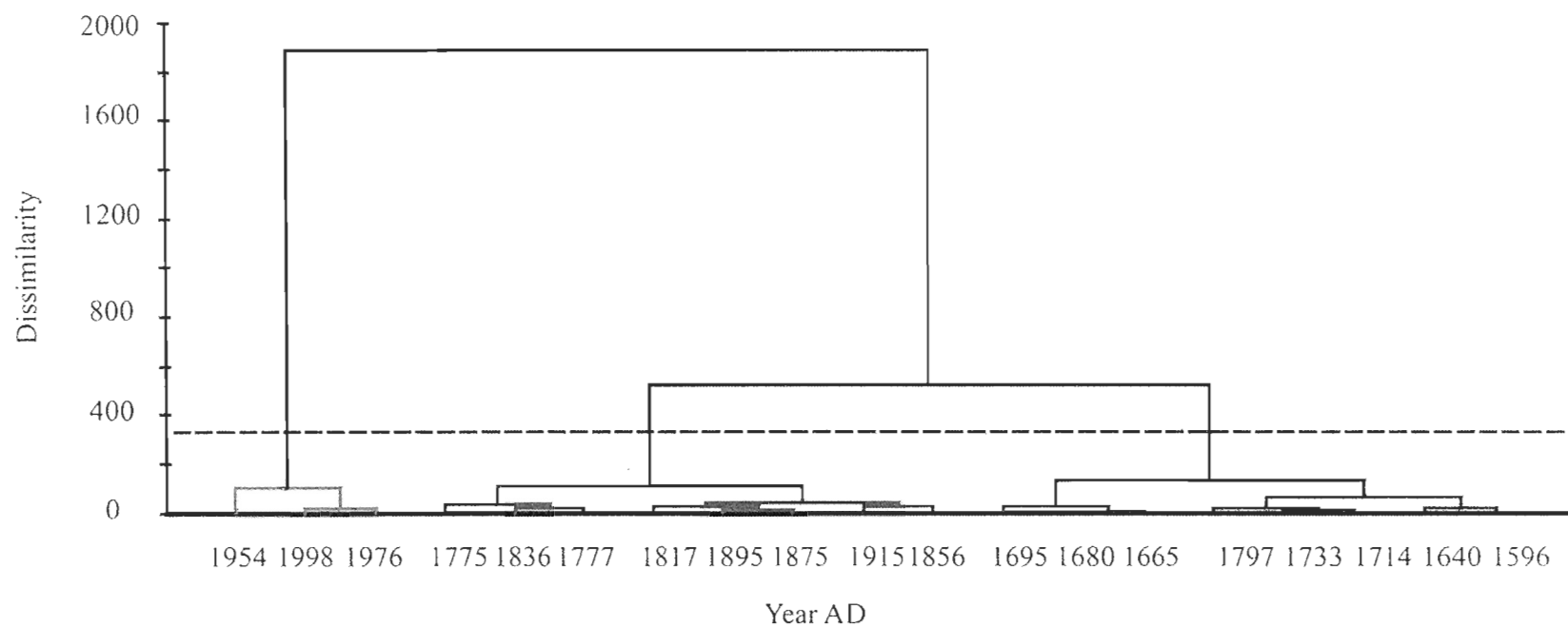
Figure 12. Dendogram dissimilarity for dinocyst assemblages

Table 5. List of organic biomarkers in HU 2008-029-040 BC-C

Organic biomarkers		1998	1976	1954	1935	1915	1895	1876	1856	1837	1817	1797	1778	1756	1734	1714	1695	1680	1665	1641	1616	1597	1577	1557	1540
Sterols	Hexadecanol	44.6	41.9	39.6	33.6	99.0	36.2	0.0	46.5	38.4	43.6	33.2	39.4	33.3	33.1	34.6	35.0	34.8	42.5	27.0	36.7	40.2	48.6	67.6	141.3
	Docosanol	75.5	58.8	65.6	55.2	158.8	68.9	0.0	78.1	82.8	87.1	79.5	81.0	60.6	66.3	54.0	64.9	70.0	83.6	50.4	62.2	59.2	55.2	47.1	279.5
	Σcholesterol	173.1	307.7	256.0	105.4	311.4	173.6	0.0	175.5	180.6	147.6	180.5	132.4	88.7	174.3	141.9	168.4	201.4	214.6	120.8	146.2	155.7	160.0	152.1	657.2
	Σbrassicasterol	103.8	169.4	142.7	79.4	269.6	146.5	0.0	161.8	165.6	132.5	147.7	100.8	83.1	168.9	137.0	133.2	183.9	170.5	105.6	118.8	145.5	83.3	217.8	545.0
	ΣCampesterol	90.7	313.4	295.3	133.2	439.6	226.3	0.0	217.0	226.5	163.1	206.1	139.4	101.6	192.6	160.3	160.9	217.2	198.6	122.3	132.9	144.9	78.5	108.6	625.2
	ΣStigmasterol	48.3	60.0	70.1	38.0	111.9	56.7	0.0	50.5	73.7	41.8	47.3	30.3	26.0	34.5	25.2	35.7	48.2	48.8	25.9	35.8	88.4	27.7	56.1	148.8
	ΣSitosterol	112.1	149.5	112.6	70.9	235.5	137.2	0.0	120.7	134.8	92.7	101.6	70.4	60.6	94.9	70.4	84.7	121.1	117.1	65.9	63.3	83.5	54.7	76.7	321.3
	ΣFucosterol	56.1	72.3	92.6	51.8	194.3	74.1	0.0	71.2	75.4	67.2	67.8	53.3	36.2	54.3	53.9	53.7	71.4	65.5	43.6	58.4	67.6	55.0	83.2	237.4
	Σdinosterols	50.0	42.0	95.2	64.4	195.3	79.8	0.0	73.4	79.2	64.3	58.2	59.1	48.8	52.6	47.9	56.6	87.4	83.6	46.4	51.8	67.2	32.7	17.9	186.6
Alkane (mg eq. Standard / g c)	C11	0.00	0.41	1.93	0.26	1.50	1.35	2.06	0.31	1.08	2.19	3.82	0.45	1.85	1.27	1.14	0.25	0.55	0.38	0.35	0.00	0.55	1.32	3.96	1.73
	C12	0.00	1.78	0.00	0.61	2.25	1.41	0.00	0.00	1.55	2.40	1.21	0.11	0.96	0.25	0.09	0.00	0.00	0.00	0.10	0.00	0.00	0.37	1.12	0.00
	C13	0.00	12.73	0.37	1.54	3.11	1.85	0.56	0.71	2.16	2.10	2.87	0.18	6.07	3.60	0.68	0.00	0.00	0.00	0.93	0.08	0.00	4.44	5.08	2.09
	C14	0.38	30.47	0.26	4.89	11.28	6.85	0.29	2.23	17.13	16.14	5.14	1.43	10.52	4.97	4.31	0.17	0.12	0.19	6.36	0.96	0.14	2.12	7.68	13.03
	C15	0.35	7.90	0.30	6.21	10.60	8.13	0.71	1.53	5.76	4.38	5.44	0.79	4.27	3.91	2.87	0.21	0.22	0.40	2.22	0.95	0.30	3.65	3.74	9.26
	C16	1.49	46.21	1.78	8.11	20.81	13.33	2.96	17.03	25.92	20.58	11.16	4.79	15.51	10.30	24.39	5.16	3.73	1.05	21.77	17.42	1.64	7.07	15.28	59.08
	C17	4.14	16.86	4.81	14.23	21.73	18.35	7.33	8.65	10.12	8.99	9.99	4.62	11.28	10.05	10.96	4.15	4.39	5.72	7.48	10.09	4.57	11.47	10.40	34.99
	Pristane	1.83	5.11	1.63	2.88	3.31	3.25	2.11	2.81	2.95	2.67	2.06	1.47	5.37	3.36	5.08	4.28	4.35	1.03	1.74	2.35	1.34	1.74	2.39	9.46
	C18	20.38	48.60	15.31	25.94	28.43	23.69	32.19	62.36	71.83	56.33	43.09	31.52	47.59	34.93	66.60	55.40	56.28	14.29	45.98	70.50	20.97	23.35	53.57	161.9
	Phytan	4.46	10.16	5.18	5.18	20.46	12.17	6.34	6.48	5.83	4.17	5.78	3.77	0.18	0.00	0.00	6.95	0.00	0.00	0.00	0.00	0.10	0.37	0.17	0.62
	C19	9.61	14.82	9.13	9.44	11.15	9.10	17.59	22.52	25.28	19.75	17.16	13.87	4.12	3.12	4.66	2.99	4.02	4.05	2.82	4.89	2.44	2.64	2.51	10.31
	C20	4.11	8.42	3.67	3.35	5.69	4.41	5.83	5.86	6.28	4.94	4.84	4.63	5.97	5.16	9.01	6.16	7.62	4.54	5.14	3.07	3.91	4.33	6.38	18.13
	C21	4.27	6.69	4.85	4.19	6.81	5.20	12.12	6.83	8.94	8.76	5.75	8.14	9.32	10.35	10.01	6.23	8.59	10.79	6.28	8.95	7.62	8.25	7.42	21.78
	C22	1.67	2.42	1.35	0.00	1.30	1.03	2.59	0.00	4.07	3.24	3.39	2.20	0.00	0.00	6.13	4.61	6.97	2.61	4.83	5.35	3.06	2.06	4.78	10.00
	C23	15.67	13.70	12.74	11.26	14.59	11.22	20.73	11.48	11.03	9.82	10.00	11.21	0.69	0.57	0.89	0.00	0.85	0.00	0.00	0.00	0.96	0.62	0.64	2.65
	C24	13.08	8.67	8.91	8.01	10.08	7.91	12.49	5.91	5.67	5.07	0.00	6.86	8.11	5.35	5.77	5.57	7.19	6.99	4.80	7.29	6.90	5.97	6.06	18.39
	C25	3.95	4.06	3.76	3.59	4.17	3.24	8.17	3.12	3.24	3.25	3.60	3.94	1.37	12.75	11.52	11.05	15.12	16.61	9.76	15.14	17.38	13.62	12.97	41.71
	C26	11.75	7.43	8.09	6.44	9.03	6.43	12.29	5.62	5.41	5.09	13.58	6.70	6.84	6.22	5.89	5.58	7.48	8.62	5.07	7.81	9.76	7.77	6.95	23.01
	C27	21.42	15.37	18.70	13.61	20.29	13.71	32.03	15.23	13.31	13.18	15.44	16.65	0.00	15.87	15.35	15.11	21.70	22.15	13.90	21.36	22.56	16.97	16.71	56.35
	C28	9.29	5.72	6.57	5.37	7.32	4.73	11.33	5.41	4.89	4.45	5.35	5.53	0.62	0.00	0.69	0.00	0.78	1.13	0.52	0.73	0.66	0.66	0.70	2.00
	C29	32.42	24.84	30.51	23.26	33.51	21.92	50.21	26.34	17.51	21.92	18.88	26.46	2.80	2.44	2.23	2.03	2.10	3.05	1.62	2.88	3.17	3.04	2.88	6.92
	C30	6.76	5.72	5.52	4.19	5.63	3.82	9.11	4.53	4.12	3.50	3.93	4.90	3.96	4.87	4.21	4.61	6.35	6.91	3.72	5.94	7.55	5.05	4.45	18.13
	C31	3.73	3.10	2.02	1.49	2.35	1.01	3.80	0.00	2.06	1.53	1.77	1.87	1.27	1.52	1.50	1.86	2.18	2.92	1.35	2.17	2.07	1.70	1.74	5.68
	C32	9.45	9.44	9.48	7.25	10.07	7.27	15.89	7.85	6.82	7.12	6.82	7.76	0.00	0.00	0.46	0.00	0.37	0.00	0.00	0.63	0.36	0.00	0.00	0.00
	C33	0.00	0.00	0.00	0.00	0.00	0.00	0.00	0.00	0.00	0.00	0.00	0.00	1.91	4.97	1.54	6.56	17.65	20.79	4.92	4.76	6.68	4.62	4.34	21.08
	C34	0.00	0.00	0.00	0.00	0.00	0.00	0.00	0.00	0.00	0.00	0.00	0.00	5.36	5.84	5.93	5.05	8.29	8.11	4.48	6.71	6.38	6.58	6.23	18.71
	C36	0.70	0.00	0.00	0.00	0.00	0.00	0.00	0.00	0.85	0.73	0.16	1.06	0.00	0.00	0.00	0.00	0.00	0.00	0.00	0.00	0.00	0.00	0.00	0.00
HBI	IP25	3.37	3.38	3.56	3.02	3.68	2.92	1.74	2.65	2.87	2.62	1.32	1.84	---	1.85	3.13	2.04	1.47	1.64	2.56	1.86	1.90	2.98	---	3.16
	HMW/LMW*	1.14	0.38	1.11	0.65	0.55	0.50	1.09	0.43	0.31	0.40	0.57	0.76	0.21	0.63	0.33	0.46	0.76	1.69	0.44	0.52	1.39	0.86	0.51	0.54

RÉFÉRENCES BIBLIOGRAPHIQUES

ACIA. 2004. *Impact of a warming arctic*. Cambrigde University Press: Cambrigde.

Axford Y, Andresen CS, Andrews JT, Belt ST, Geirsdottir A, Massé G, Miller GH, Olafsdottir S, Vare LL. 2011. Do paleoclimate proxies agree? A test comparing 19 late Holocene climate and sea-ice reconstructions from Icelandic marine and lake sediments. *Journal of Quaternary Science* **26**: 645-656.

Barber D, Marsden R, Minnett P, Ingram G, Fortier L. 2001. Physical processes within the North Water (NOW) Polynya. *Atmosphere-Ocean* **39**: 163-166.

Belicka LL, Macdonald RW, Harvey HR. 2009. Trace element and molecular markers of organic carbon dynamics along a shelf-basin continuum in sediments of the western Arctic Ocean. *Marine Chemistry* **115**: 72-85.

Belicka LL, Macdonald RW, Yunker MB, Harvey HR. 2004. The role of depositional regime on carbon transport and preservation in Arctic Ocean sediments. *Marine Chemistry* **86**: 65-88.

Belt ST, Massé G, Rowland SJ, Poulin M, Michel C, LeBlanc B. 2007. A novel chemical fossil of palaeo sea ice: IP25. *Organic Geochemistry* **38**: 16-27.

Bindschadler R. 2006. Hitting the Ice Sheets Where It Hurts. *Science* **311**: 1720-1721.

Blumer M, Mullin MM, Guillard RRL. 1970. A polyunsaturated hydrocarbon (3, 6, 9, 12, 15, 18-heneicosahexaene) in the marine food web. *Marine Biology* **6**: 226-235.

Blumer M, Guillard RRL, Chase T. 1971. Hydrocarbons of marine phytoplankton. *Marine Biology* **8**: 183-189.

Booth BC, Larouche P, Bélanger S, Klein B, Amiel D, Mei ZP. 2002. Dynamics of Chaetoceros socialis blooms in the North Water. *Deep Sea Research Part II: Topical Studies in Oceanography* **49**: 5003-5025.

Burns KA, Hernes PJ, Brinkman D, Poulsen A, Benner R. 2008. Dispersion and cycling of organic matter from the Sepik River outflow to the Papua New Guinea coast as determined from biomarkers. *Organic Geochemistry* **39**: 1747-1764.

Calvert SE, Nielsen B, Fontugne MR. 1992. Evidence from nitrogen isotope ratios for enhanced productivity during formation of eastern Mediterranean sapropels. *Nature* **359**: 223-225.

Conte MH, Volkman JK, Eglington G. 2004. Lipid biomarkers of haptophyta. in *The haptophyte Algae*, Green JC, Leadbeater BSC, (eds). Oxford University Press: USA. 351-377.

Costello MJ, Coll M, Danovaro R, Halpin P, Ojaveer H, Miloslavich P. 2010. A Census of Marine Biodiversity Knowledge, Resources, and Future Challenges. *PLoS ONE* **5**: e12110. 10.1371/journal.pone.0012110.

Dale B. 1996. Dinoflagellate cyst ecology: modelling and geological applications. in *Palynology: Principes and Applications*, Jansonius J, McGregor DC, (eds). ASSP foundation: Dallas. 1249-1275.

Damste JSS, et al. 2004. The Rise of the Rhizosolenid Diatoms. *Science* **304**: 584-587.

de Vernal A, Hillaire-Marcel C. 2008. Natural variability of Greenland climate, vegetation, and ice volume during the past million years. *Science* **320**: 1622-1625.

de Vernal A, Rochon A, Turon JL, Matthiessen J. 1997. Organic-walled dinoflagellate cysts: Palynological tracers of sea-surface conditions in middle to high latitude marine environments. *Geobios* **30**: 905-920.

de Vernal A, Hillaire-Marcel C, Solignac S, Radi T, Rochon A. 2008. Reconstructing Sea Ice Conditions in the Arctic and Sub-Arctic Prior to Human Observations. *Geophysical Monograph Series* **180**: 27-45.

de Vernal A, et al. 2005. Reconstruction of sea-surface conditions at middle to high latitudes of the Northern Hemisphere during the Last Glacial Maximum (LGM) based on dinoflagellate cyst assemblages. *Quaternary Science Reviews* **24**: 897-924.

de Vernal A, et al. 2001. Dinoflagellate cyst assemblages as tracers of sea-surface conditions in the northern North Atlantic, Arctic and sub-Arctic seas: the new 'n=677' data base and its application for quantitative palaeoceanographic reconstruction. *Journal of Quaternary Science* **16**: 681-698.

Dennis AH, Craig AC. 2002. DOC in the Arctic Ocean. in *Biogeochemistry of Marine Dissolved Organic Matter*, Dennis AH, Craig AC, (eds). Academic Press: San Diego. 665-683.

Drenzek NJ, Montluçon DB, Yunker MB, Macdonald RW, Eglinton TI. 2007. Constraints on the origin of sedimentary organic carbon in the Beaufort Sea from coupled molecular 13C and 14C measurements. *Marine Chemistry* **103**: 146-162.

Dunbar MJ. 1981. Physical causes and biological significance of polynyas and other open water in sea ice. in *Polynyas in the Canadian Artic*, Stirling I, Cleator H, (eds). Canadian Wildlife service: Canada. 29-43.

Eglinton TI, Eglinton G. 2008. Molecular proxies for paleoclimatology. *Earth and Planetary Science Letters* **275**: 1-16.

Evitt RW. 1985. *Sporopollenin Dinoflagellate Cysts - Their Morphology and Interpretation*. American association of stratigraphic palynologists foundation: Dallas.

Fortier M, Fortier L, Michel C, Legendre L. 2002. Climatic and biological forcing of the vertical flux of biogenic particles under seasonal Arctic sea ice. *Marine Ecology-Progress Series* **225**: 1-16.

Ghilarov AM. 2000. Ecosystem Functioning and Intrinsic Value of Biodiversity. *Oikos* **90**: 408-412.

Giner J-L, Wikfors GH. 2011. Dinoflagellate Sterols in marine diatoms. *Phytochemistry* **72**: 1896-1901.

Gordeev VV, Martin JM, Sidorov IS, Sidorova MV. 1996. A reassessment of the Eurasian river input of water, sediment, major elements, and nutrients to the Arctic ocean. *American Journal of Science* **296**: 664-691.

Guiot J, Goeury C. 1996. 3Pbase, a software for statistical analysis of paleoecological and paleoclimatological data. *Dendrochronologia* **14**: 1-5.

Hamel D, Vernal Ad, Gosselin M, Hillaire-Marcel C. 2002. Organic-walled microfossils and geochemical tracers: sedimentary indicators of productivity changes in the North Water and northern Baffin Bay during the last centuries. *Deep Sea Research Part II: Topical Studies in Oceanography* **49**: 5277-5295.

Hautevelle Y, Michels R, Malartre F, Elie M, Trouiller A. 2007. Tracing of variabilities within a geological barrier by molecular organic geochemistry. Case of the Callovo-Oxfordian sedimentary series in the East of the Paris Basin (France). *Applied Geochemistry* **22**: 736-759.

Henderson GM. 2002. New oceanic proxies for paleoclimate. *Earth and Planetary Science Letters* **203**: 1-13.

Hikosaka K, Ishikawa K, Borjigidai A, Muller O, Onoda Y. 2006. Temperature acclimation of photosynthesis: mechanisms involved in the changes in temperature dependence of photosynthetic rate. *Journal of Experimental Botany* **57**: 291-302.

Hillaire-Marcel C, de Vernal A, Polyak L, Darby D. 2004. Size-dependent isotopic composition of planktic foraminifers from Chukchi Sea vs. NW Atlantic sediments - implications for the Holocene paleoceanography of the western Arctic. *Quaternary Science Reviews* **23**: 245-260.

Holland DM, Thomas RH, de Young B, Ribergaard MH, Lyberth B. 2008. Acceleration of Jakobshavn Isbrae triggered by warm subsurface ocean waters. *Nature Geosci* **1**: 659-664.

IPCC. 2007. *Bilan 2007 des changements climatique : Rapport synthèse*. GIEC: Geneva.

Jakobsson M. 2002. Hypsometry and volume of the Arctic Ocean and its constituent seas. *Geochemistry Geophysics Geosystems* **3**: 18.

Jakobsson M, Grantz A, Kristoffersen Y, Macnab R. 2003. Physiographic provinces of the arctic ocean seafloor. *Geological Society of America Bulletin* **115**: 1443-1455.

James EB, Dennis AH, Craig AC. 2002. Chapter 8 - Carbon Isotopic Composition of DOM. in *Biogeochemistry of Marine Dissolved Organic Matter*. Academic Press: San Diego. 405-453.

Joughin I, Abdalati W, Fahnestock M. 2004. Large fluctuations in speed on Greenland's Jakobshavn Isbrae glacier. *Nature* **432**: 608-610.

Kang HS, Won EJ, Shin KH, Yoon HI. 2007. Organic carbon and nitrogen composition in the sediment of the Kara Sea, Arctic Ocean during the Last Glacial Maximum to Holocene times. *Geophysical Research Letters* **34**.

Laissaoui A, Benmansour M, Ziad N, Ibn Majah M, Abril J, Mulsow S. 2008. Anthropogenic radionuclides in the water column and a sediment core from the Alboran Sea: application to radiometric dating and reconstruction of historical water column radionuclide concentrations. *Journal of Paleolimnology* **40**: 823-833.

Lasternas S, Tunin-Ley A, Ibanez F, Andersen V, Pizay MD, Lemee R. 2008. Short-term dynamics of microplankton abundance and diversity in NW Mediterranean Sea during late summer conditions (DYNAPROC 2 cruise; 2004). *Biogeosciences* **8**: 743-761.

Lavoie D, Denman KL, Macdonald RW. 2010. Effects of future climate change on primary productivity and export fluxes in the Beaufort Sea. *Journal of Geophysical Research: Oceans* **115**: C04018.

Ledu D, Rochon A, de Vernal A, St-Onge G. 2008. Palynological evidence of Holocene climate change in the eastern Arctic: a possible shift in the Arctic oscillation at the millennial time scale. *Canadian Journal of Earth Sciences* **45**: 1363-1375.

—. 2010a. Holocene paleoceanography of the northwest passage, Canadian Arctic Archipelago. *Quaternary Science Reviews* **29**: 3468-3488.

Ledu D, Rochon A, De Vernal A, Barletta F, St-Onge G. 2010b. Holocene sea ice history and climate variability along the main axis of the Northwest Passage, Canadian Arctic. *Paleoceanography* **25**.

Lewis E, Ponton D, Legendre L, Leblanc B. 1996. Springtime sensible heat, nutrients and phytoplankton in the Northwater Polynya, Canadian Arctic. *Continental Shelf Research* **16**: 1775-1781.

Lovelock JE. 1993. *La Terre est un être vivant*. Flammarion: Paris.

Marret F, Zonneveld KAF. 2003. Atlas of modern organic-walled dinoflagellate cyst distribution. *Review of Palaeobotany and Palynology* **125**: 1-200.

Marty JC, Garcia N, Rairnbault P. 2008. Phytoplankton dynamics and primary production under late summer conditions in the NW Mediterranean Sea. *Deep-Sea Research Part I-Oceanographic Research Papers* **55**: 1131-1149.

Massé G, Belt ST, Rowland SJ, Rohmer M. 2004. Isoprenoid biosynthesis in the diatoms Rhizosolenia setigera (Brightwell) and Haslea ostrearia (Simonsen). *Proceedings of the National Academy of Sciences of the United States of America* **101**: 4413-4418.

McCave IN. 2007. Chapter One Deep-Sea Sediment Deposits and Properties Controlled by Currents. Pages 19-62. Developments in Marine Geology.

McKay JL, de Vernal A, Hillaire-Marcel C, Not C, Polyak L, Darby D. 2008. Holocene fluctuations in Arctic sea-ice cover: dinocyst-based reconstructions for the eastern Chukchi Sea. *Canadian Journal of Earth Sciences* **45**: 1377-1397.

Mei ZP, Legendre L, Tremblay JÉ, Miller LA, Gratton Y, Lovejoy C, Yager PL, Gosselin M. 2005. Carbon to nitrogen (C:N) stoichiometry of the spring–summer phytoplankton bloom in the North Water Polynya (NOW). *Deep Sea Research Part I: Oceanographic Research Papers* **52**: 2301-2314.

Mejanelle L, Dachs J. 2009. Short scale (6 h) temporal variation of sinking fluxes of planktonic and terrigeneous lipids at 200m in the NW Mediterranean Sea. *Biogeosciences Discussions* **6**: 1229-1265.

Melling H, Gratton Y, Ingram G. 2001. Ocean circulation within the North Water polynya of Baffin Bay. *Atmosphere-Ocean* **39**: 301-325.

Menard HW, Smith SM. 1966. Hypsometry of Ocean Basin Provinces. *J. Geophys. Res.* **71**: 4305-4325.

Menden-Deuer S, Lessard EJ. 2000. Carbon to Volume Relationships for Dinoflagellates, Diatoms, and Other Protist Plankton. *Limnology and Oceanography* **45**: 569-579.

Meyers PA. 1997. Organic geochemical proxies of paleoceanographic, paleolimnologic, and paleoclimatic processes. *Organic Geochemistry* **27**: 213-250.

Mostajir B, Gosselin M, Gratton Y, Booth B, Vasseur C, Garneau ME, Fouilland É, Vidussi F, Demers S. 2001. Surface water distribution of pico- and nanophytoplankton in relation to two distinctive water masses in the North Water, northern Baffin Bay, during fall. *Aquatic Microbial Ecology* **23**: 205-212.

Mouradian M, Panetta RJ, de Vernal A, Gelinas Y. 2007. Dinosterols or dinocysts to estimate dinoflagellate contributions to marine sedimentary organic matter? *Limnology and Oceanography* **52**: 2569-2581.

Mudie PJ, Rochon A. 2001. Distribution of dinoflagellate cysts in the Canadian Arctic marine region. *Journal of Quaternary Science* **16**: 603-620.

Mudie PJ, Rochon A, Prins MA, Soenarjo D, Troelstra SR, Levac E, Scott DB, Roncaglia L, Kuijpers A. 2006. Late Pleistocene-Holocene Marine Geology of Nares Strait Region: Palaeoceanography from Foraminifera and Dinoflagellate Cysts, Sedimentology and Stable Isotopes. *Polarforschung* **74**: 169-183.

Mueller-Lupp T, Bauch HA, Erlenkeuser H, Hefter J, Kassens H, Thiede J. 2000. Changes in the deposition of terrestrial organic matter on the Laptev Sea shelf during the Holocene: Evidence from stable carbon isotopes. *International Journal of Earth Sciences* **89**: 565-568.

Muller J, Wagner A, Fahl K, Stein R, Prange M, Lohmann G. 2011. Towards quantitative sea ice reconstructions in the northern North Atlantic: A combined biomarker and numerical modelling approach. *Earth and Planetary Science Letters* **306**: 137-148.

Nagel B, Gaye B, Kodina LA, Lahajnar N. 2009. Stable carbon and nitrogen isotopes as indicators for organic matter sources in the Kara Sea. *Marine Geology* **266**: 42-51.

Overland JE, Wang M, Salo S. 2008. The recent Arctic warm period. *Tellus Series a-Dynamic Meteorology and Oceanography* **60**: 589-597.

Parmesan C. 2006. Ecological and evolutionary responses to recent climate change. *Annual Review of Ecology Evolution and Systematics* **37**: 637-669.

Perner K, Moros M, Jennings A, Lloyd JM, Knudsen KL. 2012. Holocene palaeoceanographic evolution off West Greenland. *The Holocene*.

Peters KE, Walters CC, Moldowan JM. 2005. *The biomarker guide*. Cambridge University Press: Cambridge.

Popper K. 1963. Science as Falsification. in *Conjectures and Refutations*, Schick T, (ed). Routledge and Keagan Paul: London. 33-39.

CO2Now.org. 2013. http://co2now.org/ [April 10, 2013

Radi T, de Vernal A. 2008. Dinocysts as proxy of primary productivity in mid-high latitudes of the Northern Hemisphere. *Marine Micropaleontology* **68**: 84-114.

Radi T, et al. 2013. Operational taxonomy and (paleo-)autecology of round, brown, spiny dinoflagellate cysts from the Quaternary of high northern latitudes. *Marine Micropaleontology* **98**: 41-57.

Richerol T, Rochon A, Blasco S, Scott DB, Schell TM, Bennett RJ. 2008. Distribution of dinoflagellate cysts in surface sediments of the Mackenzie Shelf and Amundsen Gulf, Beaufort Sea (Canada). *Journal of Marine Systems* **74**: 825-839.

Rigor IG, Wallace JM. 2004. Variations in the age of Arctic sea-ice and summer sea-ice extent. *Geophysical Research Letters* **31**: 4.

Rochon A, de Vernal A. 1994. Palynomorph distribution in Recent sediments from the Labrador Sea. *Canadian Journal of Earth Sciences* **31**: 115-127.

Rochon A, Eynaud F, de Vernal A. 2008. Dinocysts as tracers of hydrographical conditions and productivity along the ocean margins: Introduction. *Marine Micropaleontology* **68**: 1-5.

Rochon A, de Vernal A, Turon J-L, Matthiessen J, Head M, J. 1999. Distribution of Recent Dinoflagellate cysts in surface sediments from the North Atlantic Ocean and adjacent seas in relation to sea-surface parameters. *AASP Contributions series* **35**: 150.

Rontani JF, Harji R, Volkman JK. 2007. Biomarkers derived from heterolytic and homolytic cleavage of allylic hydroperoxides resulting from alkenone autoxidation. *Marine Chemistry* **107**: 230-243.

Rosell-Melé A, McClymont EL. 2007. Biomarkers as Paleoceanographic Proxies. in *Proxies in Late Cenozoic Paleoceanography*, Hillaire-Marcel C, De Vernal A, (eds). Elsevier B.V.: Germany. 441-490.

Saetre MML, Dale B, Abdullah MI, Saetre G-P. 1997. Dinoflagellate cysts as potential indicators of industrial pollution in a Norwegian Fjord. *Marine Environmental Research* **44**: 167-189.

Sakshaug E. 2004. Primary and secondary production in the Arctic Seas. in *The Organic Carbon Cycle in the Arctic Ocean*, Stein R, Macdonald RW, (eds). Springer-Verlag: Heidelberg. 57-82.

Sauer PE, Eglinton TI, Hayes JM, Schimmelmann A, Sessions AL. 2001. Compound-specific D/H ratios of lipid biomarkers from sediments as a proxy for environmental and climatic conditions. *Geochimica et Cosmochimica Acta* **65**: 213-222.

Smith Jr WO, Baumann MEM, Wilson DL, Aletsee L. 1987. Phytoplankton biomass and productivity in the marginal ice zone of the Fram Strait during summer 1984. *Journal of Geophysical Research* **92**: 6777-6786.

Sorgente D, Frignani, M., Langone, L., Ravaiolo, M. 1999. *Chronology of marine sediments. Interpretation of activity-depth profiles of ^{210}Pb and other radioactive tracers. Part 1.* Consiglio Nazionale delle Ricerche. Instituto per la Geologia Marina: Bologna.

Stroeve JC, Serreze MC, Holland MM, Kay JE, Malanik J, Barrett AP. 2011. The Arctic's rapidly shrinking sea ice cover: a research synthesis. *Climatic Change* **110**: 1005-1027.

Calib 6.1.1 Website. 2011. http://calib.qub.ac.uk/calib/ [1 April 2012]

Tappan H. 1980. *The paleobiology of the Plant Protists*. Freeman: San Francisco.

Thomas RH. 2004. Force-perturbation analysis of recent thinning and acceleration of Jakobshavn Isbrae, Greenland. *Journal of Glaciology* **50**: 57-66.

Tremblay J-É, Hattori H, Michel C, Ringuette M, Mei Z-P, Lovejoy C, Fortier L, Hobson KA, Amiel D, Cochran K. 2006. Trophic structure and pathways of biogenic carbon flow in the eastern North Water Polynya. *Progress In Oceanography* **71**: 402-425.

Versteegh GJM, Blokker P. 2004. Resistant macromolecules of extant and fossil microalgae. *Phycological Research* **52**: 325-339.

Versteegh GJM, Blokker P, Bogus KA, Harding IC, Lewis J, Oltmanns S, Rochon A, Zonneveld KAF. 2012. Infra red spectroscopy, flash pyrolysis, thermally assisted hydrolysis and methylation (THM) in the presence of tetramethylammonium hydroxide (TMAH) of cultured and sediment-derived Lingulodinium polyedrum (Dinoflagellata) cyst walls. *Organic Geochemistry* **43**: 92-102.

Volkman JK. 2003. Sterols in microorganisms. *Applied Microbiology and Biotechnology* **60**: 495-506.

Volkman JK, Barrett SM, Dunstan GA. 1994. C25 and C30 highly branched isoprenoid alkenes in laboratory cultures of two marine diatoms. *Organic Geochemistry* **21**: 407-414.

Volkman JK, Barrett SM, Dunstan GA, Jeffrey SW. 1993. Geochemical significance of the occurrence of dinosterol and other 4-methyl sterols in a marine diatom. *Organic Geochemistry* **20**: 7-15.

Wassmann P. 2004. Particulate organic carbon flux to the Arctic Ocean sea floor. in *The Organic Carbon Cycle in the Arctic Ocean*, Stein R, Macdonald RW, (eds). Springer-Verlag: Heidelberg. 101-138.

Xu Y, Jaffé R. 2007. Lipid biomarkers in suspended particles from a subtropical estuary: Assessment of seasonal changes in sources and transport of organic matter. *Marine Environmental Research* **64**: 666-678.